Continuous production of succinic acid by *Actinobacillus succinogenes*: Steady state metabolic flux variation

Michael F.A. Bradfield

28077220

CVD 800

Continuous production of succinic acid by *Actinobacillus succinogenes*: Steady state metabolic flux variation

by

Michael Ford Alexander Bradfield

Dissertation presented in partial fulfilment of the requirements for the degree of

Master of Engineering in Chemical Engineering

at the University of Pretoria

Faculty of Engineering, the Built Environment and Information Technology,

Department of Chemical Engineering,

University of Pretoria

Supervisor: Prof. W. Nicol

September 2013

Synopsis

Continuous fermentations were performed in a novel external-recycle, biofilm reactor using D-glucose and CO_2 as carbon substrates. Corn steep liquor (CSL) and yeast extract (YE) served as nitrogen sources.

In anaerobic fermentations using medium containing CSL and YE, succinic acid (SA) yields were found to be an increasing function of glucose consumption. The ratio of SA to the major by-product, acetic acid (Y_{AASA}), increased from 2.4 g g^{-1} at a glucose consumption of 15 g L^{-1}, to 5.7 g g^{-1} at a glucose consumption of 46 g L^{-1}. For medium containing no CSL, Y_{AASA} remained near 1.97 g g^{-1}, exceeding this for cases where biofilm grown on CSL-containing medium was present.

The ratio of formic acid to acetic acid (Y_{AAFA}), for CSL-containing medium, decreased from an equimolar value (0.77 g g^{-1}) at a glucose consumption of 10 g L^{-1} to zero at 46 g L^{-1} glucose consumed. In contrast, Y_{AAFA} for YE-only medium remained at 0.77 g g^{-1}. Therefore, pyruvate was metabolised solely by pyruvate-formate lyase when no CSL was present.

The highest SA yield obtained on glucose, SA titre and SA productivity were 0.91 g g^{-1}, 48.5 g L^{-1} and 9.4 g L^{-1} h^{-1}, respectively, all for medium containing CSL. Medium that included CSL significantly outperformed medium that excluded CSL, achieving 64%, 21% and 203% greater SA titres, yields on glucose and productivities respectively.

Metabolic flux analyses based on the established C_3 and C_4 metabolic pathways of *Actinobacillus succinogenes* revealed that the increase in Y_{AASA}, for CSL-containing fermentations, could not be attributed to the decrease in

formate and biomass formation, and that an additional source of reducing power was present. The fraction of reducing power (NADH) unaccounted for increased with glucose consumption, suggesting that the maintenance or non-growth metabolism encountered at higher SA titres differs from the growth metabolism. It is postulated that the additional reducing power originates from an active pentose phosphate pathway in non-growing cells or from an undetected component(s) in the fermentation medium. No major metabolic flux variations were found in fermentations that excluded CSL.

Keywords: *Actinobacillus succinogenes;* biofilm; corn steep liquor; metabolic flux analysis; succinic acid

Acknowledgements

1. Prof. Willie Nicol is thanked for his financial support towards this research, in addition to his role as an excellent supervisor.

2. The financial assistance of the National Research Foundation (NRF) towards this research is hereby acknowledged. Opinions expressed and conclusions arrived at are those of the author and are not necessarily to be attributed to the NRF.

3. Gina Shin (Microbiology and Plant Pathology, FABI, University of Pretoria) is thanked for her support in maintaining the stock cultures.

4. Carel van Heerden is thanked for his general assistance in experimental work and his insights into solving sterility issues.

Contents

List of Figures

List of Tables

Nomenclature

C_{GLe}	effective glucose concentration (g L^{-1})
C_{GLo}	glucose concentration in medium (g L^{-1})
C_i	concentration of specie j (g L^{-1} or eq L^{-1})
D	dilution rate (h^{-1})
f_{dose}	time-averaged dosing fraction of base ((time pump on) (averaging period)$^{-1}$)
f_{SA}	molar equivalent fraction of succinic acid in acids mixture (eq eq^{-1})
M_{SA}	molar mass of succinic acid (g mol^{-1})
q_{SA}	volumetric productivity of succinic acid (g L^{-1} h^{-1})
Q	volumetric flow rate (mL min^{-1})
Q_{dose}	volumetric flow rate of base (mL min^{-1})
t	time interval (s)
V	volume (mL)
vvm	volumetric flow rate of gas per reactor volume (min^{-1})
X_{tot}	total biomass content (g)

Y_{ij} yield/ratio of specie *j* on specie *i* (g *j* per g *i* or mol *j* per mol *i*)

Abbreviations

AA	acetic acid
Ac-CoA	acetyl coenzyme A
AF	antifoam
ATP	adenosine triphosphate
CDM	chemically defined medium
CoA	coenzyme A
CSL	corn steep liquor
CSYE	corn steep liquor and yeast extract mixture
DCW	dry cell weight
FA	formic acid
FDH	formate dehydrogenase
FDH-H	formate dehydrogenase activity
FHL	formate-hydrogen lyase
GL	glucose

HPLC	high-performance liquid chromatography
LA	lactic acid
MA	maleic anhydride
NADH	nicotinamide adenine dinucleotide
NADPH	nicotinamide adenine dinucleotide phosphate
OXA	oxaloacetate
PDH	pyruvate dehydrogenase
PEP	phosphoenolpyruvate
PFL	pyruvate-formate lyase
PYR	pyruvate
RI	refractive index
SA	succinic acid
TA	total acids
TCA	tricarboxylic acid
TSB	tryptone soy broth
YE	yeast extract
X	biomass

Greek letters

α	CO_2 loss associated with biomass production
ΔGL	glucose consumed (g L^{-1})
κ_x	reduction level of biomass
σ	standard deviation
γ	substrate (i.e. glucose) conversion (g g^{-1})

1. Introduction

Petroleum (crude oil) and natural gas serve as the primary raw materials for producing the majority of the products (e.g. polymers, solvents, adhesives, pharmaceuticals) and fuels (e.g. diesel, gasoline, jet fuel) of modern civilisation. These raw materials, together with O_2 and N_2 from the air, are converted firstly to primary or platform chemicals (e.g. ethylene, propylene, cumene), thereafter to secondary or commodity chemicals (e.g. styrene, acetone), then to chemical intermediates, and finally to completed products used as consumer goods. Hence a chain of production exists, involving numerous chemicals and products, which hinges on the availability of a limited set of raw materials.

Today it is somewhat common knowledge that the supply of petroleum and natural gas is finite and is nearing depletion. Furthermore, the processing and consumption of these raw materials have potentially disastrous long-term impacts on the environment (VijayaVenkata Raman, Iniyan & Goic, 2012). As a result, much focus is being placed on developing alternative means and utilising sustainable resources to produce the fuels and chemical products of modern society. An approach that is gaining momentum and displaying potential is that of the biorefinery (Fernando, Adhikari, Chandrapal et al., 2006).

Analogous to the petroleum refinery which converts petroleum and natural gas to platform and commodity chemicals, followed by final products, the goal of the biorefinery is to convert biomass into the same products using a combination of technologies and processes. One such technology is the biological conversion of a fermentable substrate (derived from biomass) into a valuable product using a microorganism or enzymes. Biomass is an agricultural commodity and can be derived as a feedstock from agricultural waste or as dedicated crops, both being sustainable resources.

Succinic acid (SA) is considered to be one of the twelve most important, large-scale bio-based chemicals by the US Department of Energy (Werpy & Petersen, 2004; Bozell & Petersen, 2010) and its production could be incorporated into a biorefinery. There is a growing body of research on biological production of succinic acid (Song & Lee, 2006) and commercial plants have recently become operational (e.g. Myriant, BioAmber, Reverdia). Despite the successes achieved thus far, there is still substantial opportunity for improving bio-based succinic acid production and developing an economically viable and competitive process.

Various biocatalysts, viewed as microbial cell factories, have been investigated for SA production. The most promising bacterial candidates are *Actinobacillus succinogenes* (Guettler, Rumler & Jain, 1999), *Anaerobiospirillum succiniciproducens* (Lee, Lee, Kwon, Lee & Chang, 2000), *Basfia succiniciproducens* (Scholten, Renz & Thomas, 2009), *Mannheimia succiniciproducens* (Oh, Lee, Park, Lee & Lee, 2008) and modified strains of *Escherichia coli* (Lin, Bennett & San, 2005). Among these, *A. succinogenes* is proving to be a strong prospect for commercial production due to its ability to produce SA naturally at high titres (Zeikus, Jain & Elankovan, 1999) and its tolerance to high acid concentrations (Lin, Du, Koutinas, Wang & Webb, 2008).

Most fermentation studies on SA production using *A. succinogenes* were performed in batch reactors. However, continuous processes allow for greater productivities and for reduced cost of biocatalyst per mass of product (Wöltinger, Karau, Leuchtenberger & Drauz, 2005), which are important factors for bio-based SA production to be competitive with conventional, oil-based technologies. Furthermore, the expected growth in the SA market will demand larger quantities of product, necessitating high-volume production capabilities.

Metabolic flux analysis can be used to assess the yield limitations of a biocatalyst under different operating conditions, and to identify and examine the influence of alternative pathways on flux distribution (Nielsen, 1998). The performance of a bioreactor is closely linked to flux distributions as it has a strong influence on yield, titre and production rate, which are important parameters in the economic viability of a process (Beauprez, De Mey & Soetaert, 2010). To date, most continuous production studies on *A. succinogenes* (Urbance, Pometto, DiSpirito & Denli, 2004; Kim, Kim, Shang, Chang, Lee & Chang, 2009) have only reported yields obtained and by-product distributions. These studies do not reconcile the results with the established metabolic network of *A. succinogenes* by analysing the metabolic flux distribution. Furthermore, the studies report variations in the product distribution but do not explore the redox implications of the variations; only Van Heerden & Nicol (2013a) have performed partial metabolic flux analyses.

Metabolic flux distribution can be best assessed in a continuous fermentation at steady state since the constant environmental conditions should ensure that metabolic flux distribution remains fixed. To date, no studies have been performed on the metabolic flux distribution of *A. succinogenes* in a continuous reactor under steady-state conditions. Such a study is important because an understanding of the environmental influences on the metabolic flux distribution of *A. succinogenes* is essential for commercialisation of a fermentation process.

The objective of this study was to investigate the metabolic flux distribution of *A. succinogenes* 130Z in a continuous, biofilm reactor and to explore the effects of medium composition and biofilm presence on the flux distribution.

Fermentations were performed in a novel, external-recycle, biofilm reactor with D-glucose as the organic carbon source, CO_2 gas as the inorganic carbon source, and yeast extract and corn steep liquor as the nitrogen sources. The pH and temperature were controlled at 6.8 (with NaOH) and 37 °C respectively. The glucose concentration varied between 30 g L^{-1} and 69 g L^{-1} and the dilution rate varied between 0.05 h^{-1} and 0.55 h^{-1}. Stainless-steel wool was used as a support surface for biofilm attachment in one fermentation.

2. Theory

2.1. Succinic acid

Succinic acid (SA), a four-carbon dicarboxylic acid (Figure 2.1), is considered one of the twelve most important bio-based platform chemicals by the US Department of Energy (Werpy & Petersen, 2004; Bozell & Petersen, 2010). SA can be used in the food, agricultural, chemicals and pharmaceuticals industries. Specifically, it can serve as a precursor for chemicals such as adipic acid, 1,4-butanediol, tetrahydrofuran, *N*-methyl pyrrolidone, 2-pyrrolidone, succinate salts and γ-butyrolactone (Song & Lee, 2006).

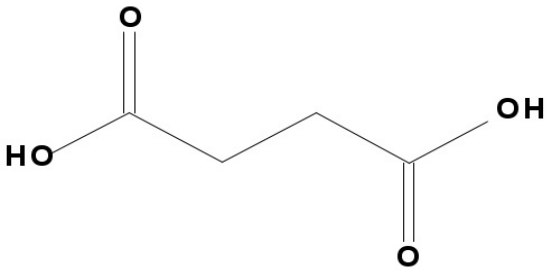

***Figure 2.1**: Succinic acid molecule ($C_4H_6O_4$)*

At present most SA is produced through a petroleum-based process by the hydrogenation of maleic anhydride (MA) or the hydration of succinic anhydride. However, the conversion cost is high, which limits the use of succinic acid (Song & Lee, 2006). The major contribution to the manufacturing cost is from MA at US$1.027 per kg SA ($Y_{MASA}$ = 0.95), whereas if glucose is used as the substrate, then the raw material cost is US$0.428 per kg SA ($Y_{GLSA}$ = 0.91).

The annual production of SA in 2009 was 30 000 tons (De Jong, Higson, Walsh & Wellisch, 2012) and it is expected to exceed 250 000 tons by 2018

(Transparency-Market-Research, 2013). The worldwide market for SA in 2012 was estimated to be worth US$240 m (Transparency-Market-Research, 2013) and it is expected to reach US$496 m by 2016 (Markets-and-Markets, 2012). In order for fermentation processes to be competitive with petrochemicals-derived products, the fermentation cost needs to be at or below US$0.55 per kg (Werpy & Petersen, 2004). Due to the high costs of and growing environmental concerns associated with the petroleum-based production of SA, and the need to shift from oil-based to renewable hydrocarbons, bio-based processes are beginning to enter the market. The following companies and joint ventures are active in the commercialisation of bio-based succinic acid: Reverdia: DSM (Netherlands) and Roquette (France) joint venture, Myriant (USA), BioAmber (USA), Succinity GmbH: BASF (Germany) and Purac (Netherlands) joint venture, and Mitsubishi (Japan).

Bio-based SA production is achieved by converting a carbohydrate substrate (i.e. glucose) to SA by means of a microbial catalyst (biocatalyst). SA is produced in the reductive branch of the tricarboxylic acid (TCA) cycle and is either a metabolic product or a metabolic intermediate. To date, several microorganisms have demonstrated potential to produce SA, with the most promising being: *Actinobacillus succinogenes* (Guettler, Jain & Rumler, 1996), *Anaerobiospirillum succiniciproducens* (Samuelov, Lamed, Lowe & Zeikus , 1991), *Basfia succiniciproducens* (Scholten et al., 2009), *Mannheimia succiniciproducens* (Lee, Lee, Hong & Chang, 2002) and modified strains of *Escherichia coli* (Beauprez et al., 2010).

In addition to the bacterial catalysts, yeast is also showing promise due to its ability to produce SA at low pH, thereby allowing SA to remain in the undissociated form, thus reducing the recovery costs of SA (Reverdia, 2011). With regard to the bacteria, *A. succinogenes* is especially promising due to its

ability to produce SA naturally at high titres (Zeikus et al., 1999; Guettler, Jain & Soni, 1998) and its high acid tolerance (Lin et al., 2008).

2.2. *Actinobacillus succinogenes*

2.2.1. Organism

A. succinogenes is a non-motile, Gram-negative, non-spore-forming, chemo-organotroph bacterium isolated from bovine rumen that occurs as rod or coccobacillus shapes (Guettler et al., 1999). As a mesophilic, facultative anaerobe (Guettler et al., 1999), *A. succinogenes* grows optimally at moderate temperatures (37 °C to 39 °C) and can survive in the presence or absence of oxygen. Furthermore, it is capnophilic as its growth is enhanced at increased CO_2 concentrations (Guettler et al., 1999). *A. succinogenes* grows between pH 6.0 and pH 7.4 and its major metabolites are succinate, acetate and formate, with ethanol produced in minor amounts (Van der Werf, Guettler, Jain & Zeikus, 1997). Although the pathogenicity of *A. succinogenes* has not been explicitly ruled out, McKinlay, Shachar-Hill, Zeikus & Vieille (2010) report that genomic sequencing suggests pathogenicity to be unlikely.

2.2.2. Metabolic network

In *A. succinogenes*, glucose is metabolised via glycolysis to two molecules of phosphoenolpyruvate (PEP), generating two molecules of nicotinamide adenine dinucleotide (NADH) (Figure 2.2). PEP serves as the node between the reverse (or reductive) branch of the TCA cycle (C_4 pathway) and fermentative metabolism (C_3 pathway).

C_4 pathway

In SA production it is desirable to channel carbon flux to the C_4 pathway as the C_3 pathway produces unwanted by-products (acetate and formate). The first

stage of the C_4 pathway involves the conversion of PEP to oxaloacetate (OXA) by PEP carboxykinase. One molecule of CO_2 is absorbed per molecule of PEP converted. CO_2 levels regulate the PEP carboxykinase pathway (Van der Werf et al., 1997), which is essential in succinic acid production. It is therefore important to achieve the correct extracellular and intracellular CO_2 levels during SA production.

OXA is then reduced to L-malate by malate dehydrogenase, consuming one molecule of NADH. Thereafter fumarate is formed in the conversion of L-malate by fumarase. The final step in SA production involves the reduction of fumarate to succinate by fumarate reductase; one molecule of NADH is consumed. Therefore, two molecules of NADH are converted to NAD^+ along the reductive branch of the TCA cycle in SA formation.

C_3 pathway

Instead of PEP being converted to OXA, it can be converted to pyruvate (PYR) by pyruvate kinase. PYR serves as the start of the C_3 pathway and is an important branch point (or node) in flux analysis. It can be converted to acetyl-CoA (Ac-CoA) by pyruvate dehydrogenase (PDH) or pyruvate-formate lyase (PFL).

Conversion with PDH[1] results in the liberation of one molecule of CO_2 and NADH. Alternatively, if PYR is converted to Ac-CoA by PFL,[2] formate is produced instead of CO_2 and NADH. Therefore, no gain in NADH is achieved,

[1] PDH is part of the pyruvate dehydrogenase complex (PDH) which uses thiamine pyrophosphate, lipoate and CoA as cofactors (Spector, 2009: 252). Thiamine pyrophosphate is a derivative of thiamine (vitamin B_1) produced by thiamine pyrophosphatase.
[2] In *E. coli*, PFL exists in three forms: active, inactive and irreversibly inactive. The enzyme is activated post-translationally by means of an iron-dependent activating enzyme (Wagner, Frey, Neugebauer, Schäfer, & Knappe, 1992). The enzyme is oxygen-sensitive as exposure to oxygen results in irreversible inactivation (Knappe, Neugebauert, Blaschkowski & Ganzler, 1984).

in contrast to the conversion using PDH. PFL is active only during anaerobic fermentations as it is deactivated in the presence of O_2.

It is possible for formate to be broken down by formate dehydrogenase (FDH), resulting in the formation of CO_2 and NADH. Therefore, if FDH[3] is active together with PFL, it is possible to achieve the same NADH gain as with PYR conversion by PDH.

Ac-CoA serves as a branch point between ethanol and acetate. Acetate is produced by the conversion of Ac-CoA to acetyl-phosphate by acetate kinase, followed by the conversion of acetyl-phosphate using phosphotransacetlyase. In ethanol formation, Ac-CoA is converted to acetaldehyde using acetaldehyde dehydrogenase and one molecule of NADH. Acetaldehyde is then converted to ethanol by alcohol dehydrogenase, consuming one molecule of NADH. In the absence of ethanol production, the C_3 pathway can at best deliver one molecule of NADH.

[3] Formate dehydrogenase activity (FDH-H) is present in the enzyme complex formate hydrogen lyase (FHL). In FHL, CO_2 is generated by the FDH activity and is encoded by the *fdhF* gene. The H_2 is formed by a hydrogenase-3 activity and the reaction occurs only in the absence of an electron acceptor (O_2 or nitrate) and the presence of formate and the cofactor molybdate. The expression of *fdhF* appears to require acidic conditions and the expression of PFL, FDH-H and hydrogenase-3 all increase under carbon substrate starvation (Spector, 2009: 257).

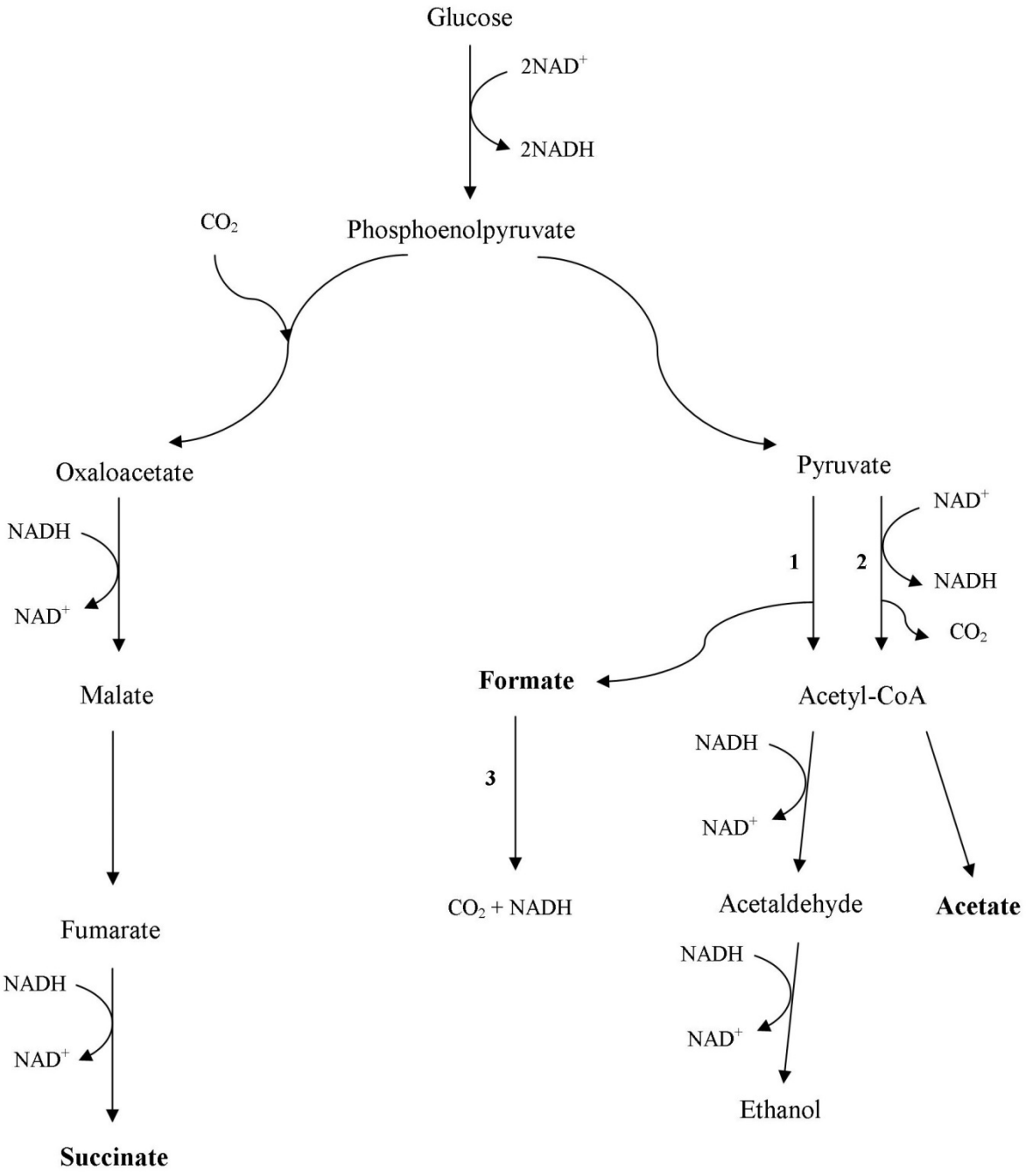

***Figure 2.2**: Simplified metabolic network of A. succinogenes showing the pathways leading to its major metabolites and redox flow (based on McKinlay, Laivenieks, Schindler et al. (2007)). The relevant enzymes are (1) pyruvate-formate lyase, (2) pyruvate dehydrogenase and (3) formate dehydrogenase. ATP flow is excluded.*

2.2.3. Production studies

Various studies on the production of SA using *A. succinogenes* have been done to assess the viability of using the organism as an industrial biocatalyst. From Table 2.1 it can be seen that the highest yield of SA on glucose and the highest SA titre achieved in continuous fermentations are 0.76 g g^{-1} and 18.6 g L^{-1} respectively. The highest yield and SA titre achieved in batch fermentations (Table 2.2) are 0.94 g g^{-1} and 79 g L^{-1} respectively. However, the maxima achieved for batch studies used *A. succinogenes* NJ113. To date, no experimental comparison of strains 130Z and NJ113 has been performed.

***Table 2.1**: Significant continuous fermentation studies performed with A. succinogenes 130Z*

Study	Medium †	C_{SA}* (g L^{-1})	Y_{GLSA}* (g g^{-1})	Y_{AASA}* (g g^{-1})	Y_{AAFA}* (g g^{-1})	q_{SA} (g L^{-1} h^{-1})
(Urbance et al., 2004)	YE;CSL	10.4	**0.76**	-	-	**8.8**
(Kim, Kim, Shang, Chang, Lee, & Chang , 2009)	YE	**18.6**	0.59	**2.8**	0.78	6.6
(Van Heerden & Nicol, 2013a)	YE;CSL	13.0	0.71	2.5	**0.77**	6.4

*Only the best results for each study are reported. Therefore the yields and concentrations are not necessarily from the same fermentation.

† Only fermentations using glucose as the organic carbon source are considered.

The highest ratios of succinate to acetate achieved in continuous fermentations and batch fermentations are 2.8 g g^{-1} and 15.3 g g^{-1} respectively. The lowest ratio of formate to acetate reported for continuous fermentations is 0.77 g g^{-1}, while that for batch studies is zero.

***Table 2.2**: Significant batch fermentation studies performed with A. succinogenes 130Z and A. succinogenes NJ113*

Study	Strain	Medium†	C_{SA} (g L^{-1})	Y_{GLSA} (g g^{-1})	Y_{AASA} (g g^{-1})	Y_{AAFA} (g g^{-1})
(Guettler et al., 1996)	130Z	YE;CSL	67	0.68	5.6	0.69
(Guettler et al., 1998)	130Z	YE;CSL	**79**	0.79	-	-
(Urbance, Pometto, DiSpirito & Demirci, 2003)	130Z	YE;CSL	17.4	0.87	-	-
(Corona-González, Bories, González-Álvarez & Pelayo-Ortiz, 2008)	130Z	YE	33.8	0.62	5.2	0.81
(Xi, Chen, Xu, Zhang, Bai, Jiang, Wei & Chen, 2012)	NJ113	CDM*	42.3	**0.94**	**15.3**	**0**
(Xi, Chen, Dai, Ma, Zhang, Jiang, Wei, & Ouyang, 2013)	NJ113	CSL;heme	37.9	0.82	8.9	0.61
		CSL	24.7	0.70	7.9	0.69

*CDM = chemically defined medium

†Only fermentations using glucose as the organic carbon source are considered.

2.2.4. Fermentation medium studies

An important factor in microbial fermentations is the choice and composition of the fermentation medium. The medium should contain all the necessary nutrients that the chosen biocatalyst requires for growth and sustenance. Furthermore, the cost of the fermentation medium is an important consideration in industrial fermentations.

Nitrogen, a constituent of proteins, nucleic acids and coenzymes, is essential for the growth of microorganisms. The choice of a nitrogen source is therefore an important consideration in fermentations with *A. succinogenes*. At present, the literature suggests that the most promising candidates are yeast extract (YE) and corn steep liquor (CSL). These candidates also include various vitamins, amino acids, minerals and trace metals that are either essential for, or facilitate, the growth of *A. succinogenes* as it is auxotrophic.

In batch fermentations with *A. succinogenes*, higher yields, succinate titres and flux to SA were achieved with media containing CSL instead of only YE (Table 2.2). The highest yield and flux to SA was achieved with a chemically defined medium (Xi et al., 2012), while the best SA titre was achieved with a mixed (CSL and YE) medium (Guettler et al., 1998). Results from continuous fermentations do not conclusively favour the use of CSL over YE (Table 2.1), but the SA yields on glucose for the mixed medium runs were higher than those obtained for the fermentation using only YE.

McKinlay et al. (2010) determined the essential vitamins required for the growth of *A. succinogenes* to be: nicotinic acid, pantothenate, pyridoxine and thiamine, and the required amino acids to be: cysteine, glutamate and methionine. However, they report that *A. succinogenes* is able to synthesise

cysteine from sulphide or thiosulphate, but not from sulphate. Furthermore, they determined that several genes involved in biotin synthesis are absent, yet it is able to grow without biotin supplementation. By contrast, Xi et al. (2012) determined the essential vitamins to be only biotin and nicotinic acid, and the essential amino acids to be only glutamate and methionine.

In addition, Xi et al. (2012) investigated the influence of biotin on the growth of *A. succinogenes* and SA production by varying the biotin concentration in a chemically defined medium. Without biotin, cell growth was severely inhibited and no SA was produced. However, the reported data regarding C_{AA}, Y_{GLAA} and Y_{AASA} are inconsistent. For example, in the experiment using 10 mg L^{-1} biotin, the glucose consumed is 30.0 g L^{-1}, C_{SA} = 18.7 g L^{-1}, C_{AA} = 2.9 g L^{-1}, Y_{GLAA} = 0.213 g g^{-1} and Y_{AASA} = 6.4 g g^{-1}. From this, the calculated Y_{GLAA} is 0.097 g g^{-1}, but using the reported Y_{AASA} value instead of the C_{AA} value in the calculation yields the correct Y_{GLAA} value. It is possible that the Y_{AASA} and C_{AA} values have been switched since the same inconsistency occurs for all the biotin data.

2.3. Metabolic flux distribution

Metabolic pathways consist of a series of enzymatic reactions that occur within living cells and are essential in the maintenance of homeostasis within an organism. A metabolic pathway converts a substrate (e.g. glucose) to a final product (e.g. succinate) that can either be used immediately by the organism, used to initiate another metabolic pathway or can be stored within the cell. The carbon in the substrate can all form part of the final product or it can be channelled to diverging pathways. Carbon can also enter the pathway from converging pathways, and any intermediates produced in a metabolic pathway may be excreted by the cell.

Metabolic pathways also have associated redox and energy flows. It is useful to use NADH and adenosine triphosphate (ATP) as the redox and energy currencies (Villadsen, Nielsen & Lidén, 2011: 19) respectively. To simplify balances, nicotinamide adenine dinucleotide phosphate (NADPH) can be viewed as NADH.

Metabolic flux

Metabolic flux is the rate of flow of carbon (or metabolites) along a specific metabolic pathway. Maximising carbon flux to the desired metabolite is important for the economic viability of a fermentation process since it influences yield, product titre and productivity – key parameters in optimising a bioreactor. To analyse flux distribution it is important to have an idea of the metabolic network that is active within an organism.

Flux distribution can be manipulated by genetically modifying an organism by engineering specific pathways or by deleting unwanted pathways. A potential downfall of this is reversion of the modified strain to the less-productive

wild-type strain, a well-known problem in industry (Villadsen et al., 2011: 434). Wild-type strains that are naturally good producers of the desired product do not face such a problem. Flux in wild-type strains can be manipulated by providing the appropriate environmental conditions to ensure that carbon flux to the pathway producing the desired product is favoured. It may also be possible to supplement the fermentation medium with components that facilitate carbon flux to the desired product. For example, providing electrically reduced neutral red improved SA yields and product ratios with *A. succinogenes* by serving as an electron donor (Park & Zeikus, 1999), and flux to SA increased with increasing H_2 and CO_2 concentrations (Van der Werf et al., 1997).

Metabolic flux analysis

Flux analysis is a framework for analysing the flow of carbon through various pathways in a metabolic network. Intracellular fluxes are calculated by using a stoichiometric model for all the major intracellular reactions and applying mass balances around the intracellular metabolites (Nielsen, 1998). The following constraints can be imposed on a metabolic network to solve for fluxes (Villadsen et al., 2011: 155):

1. The relationships between internal fluxes
2. A total carbon balance between the products and the substrate
3. A redox balance between that consumed and that produced, based on NADH
4. An energy balance based on ATP generation and consumption.

To compare the extent of flux between different pathways it is useful to use the ratios (or relative yields) of the metabolites resulting from different pathways. The flux distribution of *A. succinogenes* can therefore be represented by the ratios of succinate to acetate (Y_{AASA}, flux at the PEP node) and formate to acetate

(Y_{AAFA}, flux at the pyruvate node) (Section 2.2.2). The yield of SA on glucose (Y_{GLSA}) serves as the final flux distribution parameter and incorporates flux to biomass. With respect to SA production, it is desirable to maximise Y_{AASA} and Y_{GLSA}.

3. Experimental

3.1. Microorganism and growth

The microorganism used in this study was *Actinobacillus succinogenes* 130Z (DSM No. 22257 or ATCC No. 55618) from the German Collection of Microorganisms and Cell Cultures (Braunschweig, Germany). Viable stocks of the organism were maintained by monthly cultivations in tryptone soy broth (TSB) at 37 °C for 16-20 h in an incubator with a shaker speed of 150 rpm. The stock cultures were stored as 15-mL broths in 25-mL screw-cap vials at 5 °C. Cultures were tested for purity and viability by preparing new 15-mL broths of TSB, inoculating with stock culture, and then analysing the broth by high-performance liquid chromatography (HPLC) after 16-24 h. If the broth contained lactic acid or ethanol, it was deemed to be contaminated, and if no succinic acid formed, the culture was deemed unviable.

3.2. Fermentation media

Two different fermentation media were used in this study: one based on yeast extract (YE) and salts – the YE-medium, the other on a mixture of YE, corn steep liquor (CSL) and salts – the CSYE-medium. All chemicals were obtained from Merck KGaA (Darmstadt, Germany) unless otherwise stated. The medium consisted of three parts: a growth medium, a phosphate buffer and a glucose solution. The CSYE-medium, based on Urbance et al. (2003), had the following composition: 6.0 g L^{-1} YE, 10.0 g L^{-1} clarified CSL, (Sigma-Aldrich, St. Louis, USA), 1.0 g L^{-1} NaCl, 0.2 g L^{-1} $MgCl_2 \cdot 6H_2O$, 0.2 g L^{-1} $CaCl_2 \cdot 2H_2O$, 1.36 g L^{-1} sodium acetate, 2.5-5 mL Antifoam A (Sigma-Aldrich, St. Louis, USA) and 0.16 g L^{-1} $Na_2S \cdot 9H_2O$ (for anaerobic conditions). The YE-medium had the same composition, except that no CSL was added and the concentration of YE was

16.0 g L^{-1}. In the initial fermentations with the YE-medium, $Na_2S{\cdot}9H_2O$ was excluded to allow for aerobic conditions.

CSL was clarified by boiling a 200 g L^{-1} solution of CSL and distilled water at 105 °C for 15 min and allowing the solids to precipitate during cooling. Once cooled, the supernatant was removed and used for the growth medium. Unused supernatant was stored at 5 °C.

The phosphate buffer consisted of 3.2 g L^{-1} KH_2PO_4 and 1.6 g L^{-1} K_2HPO_4. The D-glucose concentration varied from 30 g L^{-1} to 69 g L^{-1}. CO_2 gas (Afrox, Johannesburg, South Africa) was fed into the recycle line at between 1% vvm and 10% vvm to serve as the inorganic carbon source.

3.3. Bioreactor

Two versions of a novel bioreactor were used for the fermentations. Reactor A was used for most of the YE-medium fermentations (Figure 3.1) and Reactor B was used for all the CSYE-medium fermentations (Figure 3.2) and one YE-medium fermentation. Reactor B was developed to solve foaming and stability problems encountered in Reactor A. Excessive foaming led to washout of biofilm, making it difficult to achieve steady state.

Both reactors consisted of a glass cylinder contained between an aluminium base and head, connected by an external recycle line for agitation. In one fermentation, stainless-steel wool was placed loosely into the glass portion of Reactor B to serve as an attachment surface for biofilm. The volume of Reactor A, including the recycle line, was 137 mL and the void volume of Reactor B was 158 mL with a total volume of 179 mL. The glass body of Reactor B was incompletely filled to provide an open headspace, which assisted in foam control.

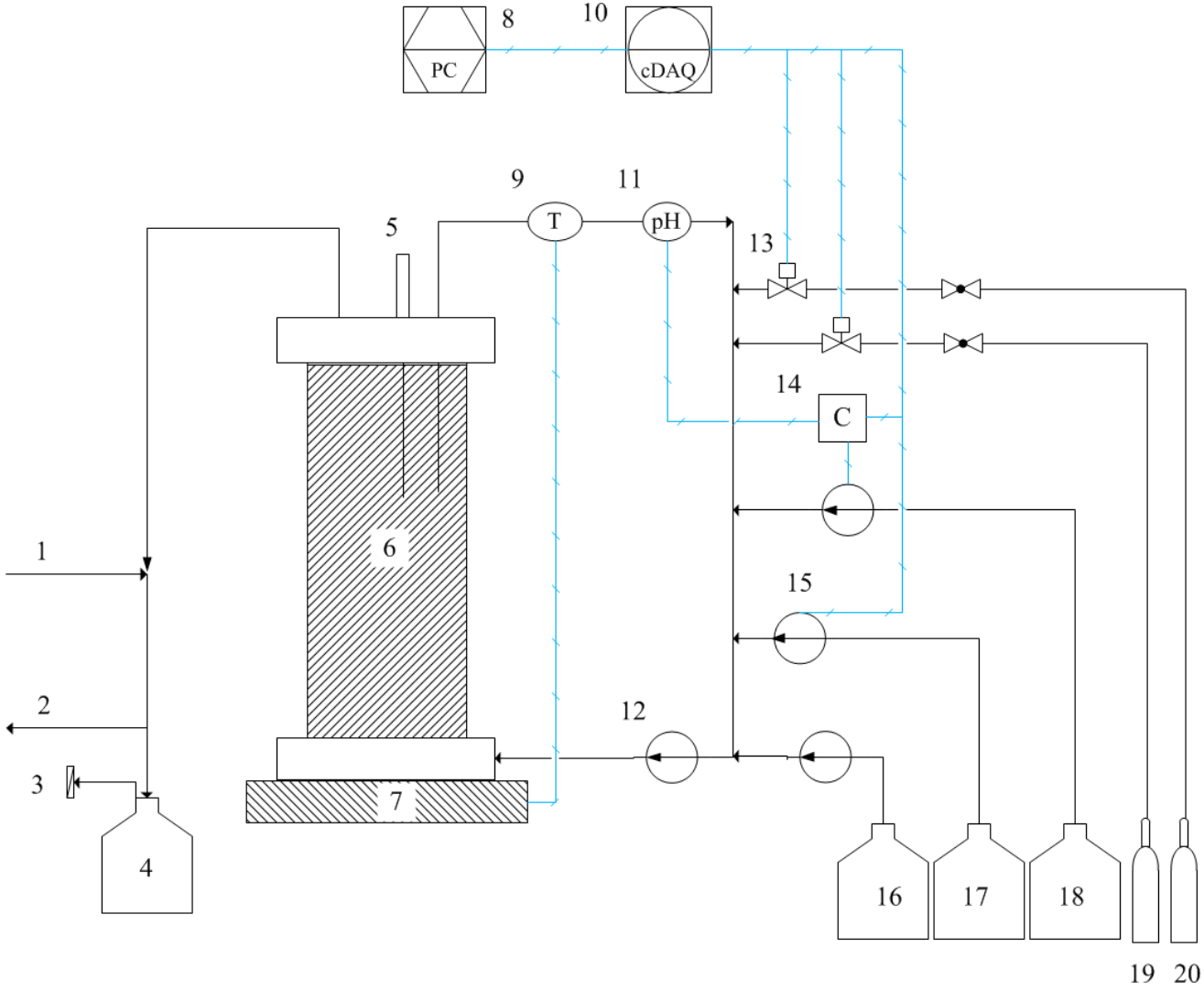

No.	Description
1	Compressed air purge
2	Sample line
3	Gas filter
4	Product reservoir
5	Inoculation septum
6	Reactor body
7	Hot plate
8	PC and interface
9	Thermocouple & temp. controller
10	cDAQ
11	pH probe
12	Recycle pump
13	Gas flow controller
14	pH controller
15	Peristaltic pump
16	Medium reservoir
17	Antifoam reservoir
18	NaOH reservoir
19	CO_2 cylinder
20	Compressed air

***Figure 3.1**: Simplified schematic of Reactor A, used for YE-medium fermentations*

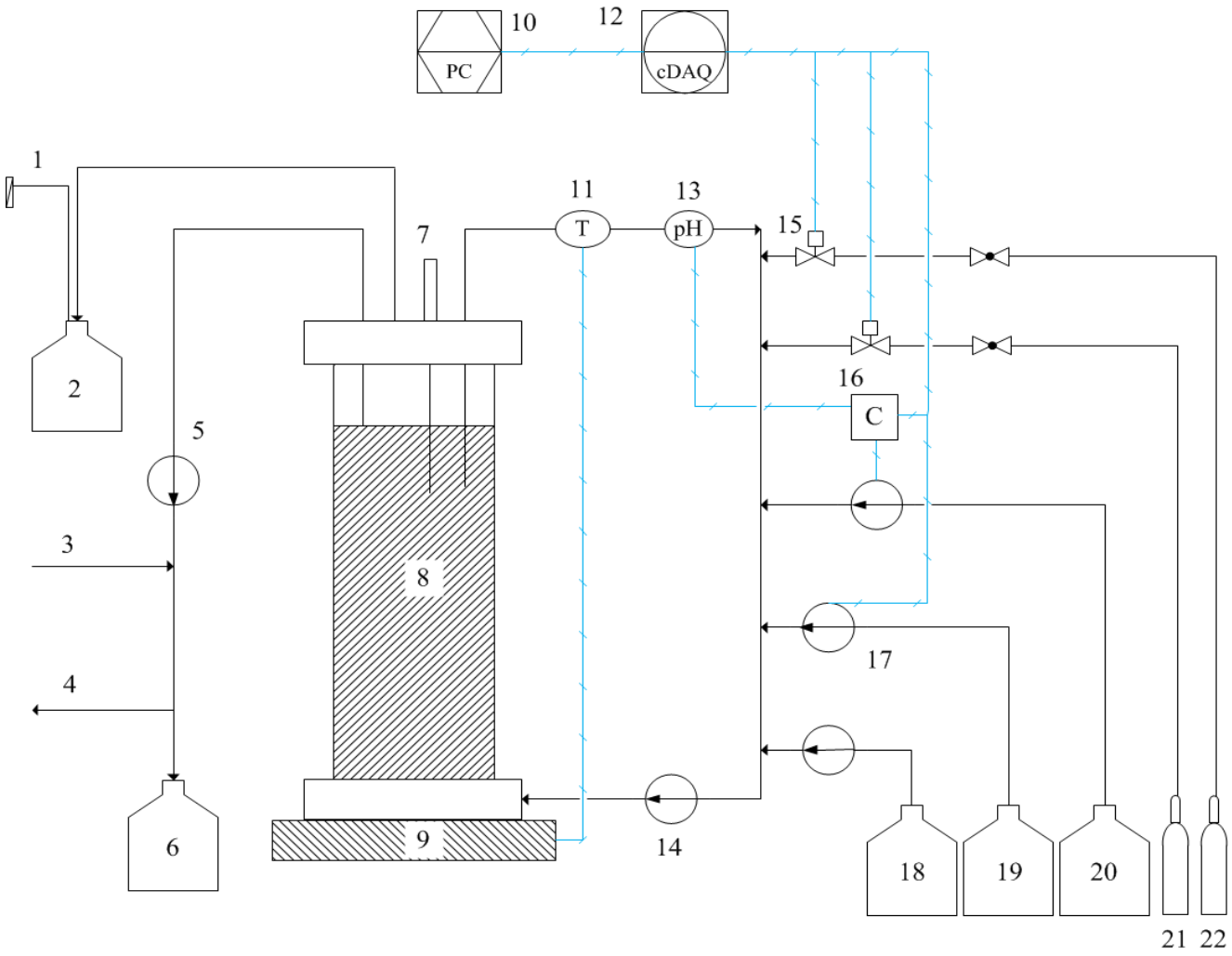

No.	Description
1	Gas filter
2	Foam-trap
3	Compressed air purge
4	Sample line
5	Peristaltic pump
6	Product reservoir
7	Inoculation septum
8	Reactor body
9	Hot plate
10	PC
11	Thermocouple & temp. controller
12	cDAQ
13	pH probe
14	Recycle pump
15	Gas flow controller
16	pH controller
17	Peristaltic pump
18	Medium reservoir
19	Antifoam reservoir
20	NaOH reservoir
21	CO_2 cylinder
22	Compressed air

Figure 3.2: *Simplified schematic of Reactor B, used for CSYE-medium runs*

All gas inlets and outlets, including reservoir vents (not shown in the figures), contained 0.2 µm PTFE membrane filters (Midisart 2000, Sartorius, Göttingen, Germany). In Reactor A, gas exited via the exit line and product bottle, while in Reactor B, gas vented via a foam trap which assisted in foam control and prevented foam from blocking the filter on the outlet. The level in Reactor A was maintained by natural overflow of effluent into the product bottle. In Reactor B, the level was maintained by using a pump on the exit line with a fixed intake point, thus controlling the level of the headspace. All pumps used in the system were peristaltic pumps.

Temperature was controlled at 37 °C by a hotplate coupled to a thermocouple connected in-line within the recycle stream. pH was measured using a Tophit CPS417D ISFET probe (Endress+Hauser, Gerlingen, Germany) housed within an aluminium holder connected in-line within the recycle stream. Control of pH at 6.8 was achieved using a Liquiline CM442 (Endress+Hauser, Gerlingen, Germany) in which an internal relay controlled the dosing of 10 M, unsterilised NaOH in an On–Off fashion. In addition to the thermocouple, temperature was measured using the pH probe for data logging purposes. Temperature and pH fluctuations are discussed in Section 3.10.

Compressed air was continuously fed through the exit line to maintain a positive pressure which assists in aseptic sampling and helps to prevent contamination of the reactor. Compressed air and CO_2 flow rates were controlled using Brooks 5850S mass flow controllers (Brooks Instrument, Hungary).

3.4. Fermentations

Five successful fermentations were performed: one using Reactor A and four using Reactor B. The durations of the fermentations are given in Table 3.1.

A total of 124 days and 15 hours of operation was achieved. Fermentations were terminated due to contaminations, system exposure (e.g. lines breaking or detaching from reactor) or as planned. Contaminations were detected by an increase in lactic acid and/or ethanol in the product stream, suggesting that lactic acid bacteria were responsible for the infiltration. The bulk of the data were generated in runs 1, 3 and 5.

***Table 3.1**: Durations of the successful fermentations*

Run number	Duration (h)	Duration (d, h)
1	533	22 d 5 h
2	90	3 d 18 h
3	968	40 d 8 h
4	17	0 d 17 h
5	1 383	57 d 15 h
TOTAL	**2 991**	**124 d 15 h**

Procedure

Fermentations were started by preparing the three parts of the fermentation medium (growth medium, buffer and glucose) in separate bottles connected to the reactor system. The entire reactor system (excluding NaOH and electrical components) was autoclaved at 121 °C for 40 min. To prevent unwanted reactions among the medium components, the three medium parts were only mixed once the system had cooled to room temperature (approx. 20 °C). The reactor was filled with medium and gas flow was established in order to create a positive pressure in the reactor. Once the temperature (37 °C) and pH (6.8) had

stabilised, 10 mL of inoculum was aseptically injected into the reactor through a silicon septum attached to the reactor head.

Fermentations were initialised by operating the system at a low dilution rate to allow cells to accumulate without the possibility of washout. Additional antifoam was dosed into the reactor when necessary. The dilution rate was varied from 0.05 h^{-1} to 0.55 h^{-1}. CO_2 flow rates were varied in the initial fermentations to determine the influence of CO_2 on the metabolic flux distribution and the minimum required CO_2 flow rate for optimal C_4 pathway flux. A vvm above 5% seemed sufficient to maintain CO_2 saturation in the reactors, although this may be insufficient at high productivities. At stages in the fermentations, air was fed into the reactor body to investigate the influence of air on the product distribution and biofilm formation. Biofilm attachment occurred on the head, base, glass and tubing of the reactor, as well as the stainless-steel wool in the case of run 5. There was also a substantial amount of biofilm on the glass perimeter of the headspace, and on and around the pH probe.

Medium replenishment

A sterile coupling (Figure 3.3) was used to transfer fresh medium into the feed reservoir online once the initial medium had been depleted. The coupling consisted of a U-connection, one half of which was fixed to the feed reservoir and the other half to the replenishment reservoir. Each half of the connection had a ball valve to isolate the system from the environment. The replenishment reservoir, containing a medium make-up the same as that of the main fermentation setup, was autoclaved at 121 °C for 40 min. Once cooled, the medium components were mixed. The half connections were then coupled and the U-connection was placed in an oil bath at 140 °C for 20 min. The medium

was then transferred from the replenishment reservoir into the main feed reservoir via the sterile coupling. After completion of the transfer, the ball valves were closed and the coupling was disconnected. Out of eleven transfers, reactor contamination occurred twice as a result of transfers, giving a success rate of 82%.

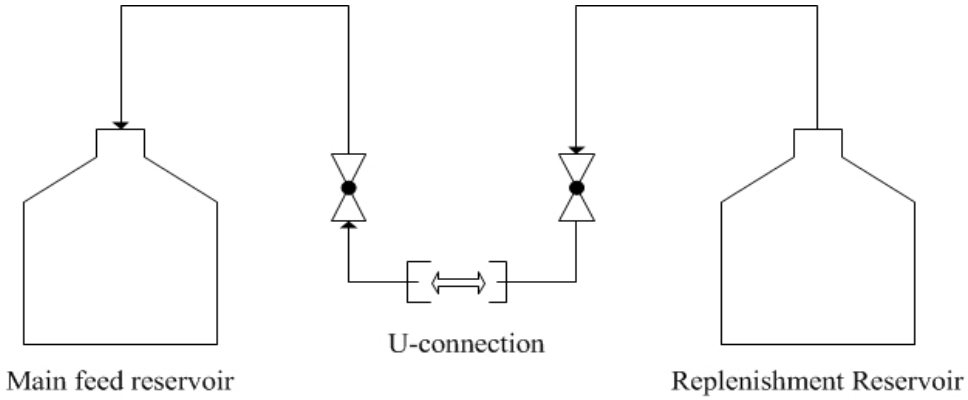

***Figure 3.3**: Schematic of the U-connection used for the online transfer of fresh medium*

3.5. Online monitoring

A custom-developed LabView (National Instruments) program was used to monitor and control the reactor. The LabView program was linked to the reactor instrumentation by means of a cDAQ-9184 data acquisition device (National Instruments, Hungary) with voltage and current input modules and a current output module. Gas flow rates and the antifoam dosing timing were set via the program. Temperature, pH, gas flow rates and the time-averaged dosing of NaOH were recorded through the program.

Once the time-averaged NaOH dosing fraction had ceased to fluctuate, implying that the rate of acids production was constant, it was assumed that the system had reached pseudo-steady state. Pseudo-steady state assumes that the concentration of the components in a cell are constant in time as the relaxation

times are either very long or very short compared with the time constants for changes in the environment (Villadsen et al., 2011: 301). Another view on this refers to the state in enzymatic reactions where the concentration of the enzyme-substrate complex is assumed to be constant in time (Segel & Slemrod, 1989).

Productivity-based steady state check

A second check for steady state was implemented late in the experimental work and was based on the volumetric productivity of SA (q_{SA}). The check involves comparing an instantaneous, predicted q_{SA} versus a q_{SA} based on the initial concentration of SA. When the system has achieved steady state, the q_{SA} based on the initial concentration of SA will equal the instantaneous q_{SA} and the two values will overlap on an online chart of productivity versus time.

The instantaneous q_{SA} is based on a predicted SA concentration which follows from the product distribution (SA, AA & FA) obtained from an HPLC analysis. The fraction of SA molar equivalents (f_{SA}) of the total acids (TA) molar equivalents produced is calculated from Equation 3.1, where Y_{SAAA} and Y_{SAFA} are the molar yields of AA and FA relative to SA respectively. The fraction is then incorporated into the productivity expression for SA (Equation 3.2) which is f_{SA} multiplied by the molar equivalent concentration of the total acids (C_{TA}).

C_{TA} at a point in time can be calculated by multiplying the time-averaged base (NaOH) dosing fraction (f_{dose}) by the flow rate of the base dosing pump (Q_{dose}) and the molar equivalent concentration of the base (C_{base}). For NaOH the molar concentration will be equal to the molar equivalent concentration. This yields an average molar equivalent flow rate of base which is equal to the TA molar equivalent productivity. Expressing q_{SA} as the product of dilution rate ($D = Q_{in}/V$) and C_{SA}, and rearranging results in Equation 3.3 which can be used to predict C_{SA} since all the variables on the right-hand side of the equation are

known. However, the product distribution is only as accurate as the most recent HPLC analysis.

$$f_{SA} = \frac{2}{2 + Y_{SAAA} + Y_{SAFA}} \quad \textbf{3.1}$$

$$q_{SA} = f_{SA} C_{TA} M_{SA} D \quad \textbf{3.2}$$

$$C_{SA_p} = 60 \left(\frac{f_{SA}(f_{dose} Q_{dose} C_{base}) M_{SA}}{Q_{in}} \right) \quad \textbf{3.3}$$

The predicted SA concentration from Equation 3.3 can now be used to calculate an estimated or predicted SA productivity, q_{SAp} (Equation 3.4).

Equation 3.5 gives the time-dependent SA mass balance for a continuous tank reactor. When the system has reached steady state, the differential term will equal zero and q_{SAp} will equal the outlet flow rate of SA. Integrating Equation 3.5 results in Equation 3.6, which is used to calculate C_{SA} based on incremental changes in the predicted productivity. In Equation 3.6 (programmed into LabView), Δt represents the sampling time of the program, C_{SA0} the initial C_{SA} (at the instant when the program is initialised) and q_{SApi} the predicted productivity from Equation 3.4 at the instant of sampling. Since the sampling interval is small (1 s) relative to the length of the fermentation, the previously calculated C_{SA} value (C_{SAi-1}) can be used on the right-hand side of Equation 3.6 to simplify the calculation.

$$q_{SA_p} = C_{SA_p} D \quad \textbf{3.4}$$

$$\frac{dC_{SA}}{dt} = q_{SA_p} - C_{SA} D \quad \textbf{3.5}$$

$$C_{SA_i} = \sum (q_{SA_{p_i}} - C_{SA_{i-1}} D)\, \Delta t + C_{SA_0} \qquad \textbf{3.6}$$

A productivity value based on the history of all the predicted values and the initial concentration of SA can now be calculated by multiplying C_{SAi} by a real-time calculation of *D*. The real-time *D* is based on the flow rate of the feed pump, the average flow rate of the dosing and antifoam pumps, and the volume of the reactor. Since the dosing fraction varies over time in a transient system, *D* is continuously updated. The two productivities can now be plotted in real-time and once the two overlap and remain stable for a noteworthy period of time, in addition to the plateauing of the dosing fraction, steady state can be assumed. To verify steady state, HPLC analyses spaced at least two volume turnovers apart were performed to assess whether product concentrations remained constant.

3.6. Analytical methods

HPLC was used to determine the concentrations of glucose, ethanol and organic acids. Analyses were performed using an Agilent 1260 Infinity HPLC (Agilent Technologies, USA), equipped with a refractive index (RI) detector and a 300 mm x 7.8 mm Aminex HPX-87 H ion-exchange column (Bio-Rad Laboratories, USA). The flow rate of the mobile phase (0.3 mL L^{-1} H_2SO_4) was 0.6 mL min^{-1} and the column temperature was 60 °C.

Dry cell weight (DCW) was determined from 9-mL samples or 24-h samples (volume of the sample dependent on dilution rate) centrifuged at 12 100 x g for 1.5 min and 3 095 x g for 10 min respectively. Cell pellets were washed twice with distilled water and centrifuged between washes, then dried at 85 °C for at least 24 h.

3.7. Data analysis and collection

The product stream of the reactor was sampled once the system had reached steady state as determined in Section 3.5. The sample was collected in a vial placed in ice to ensure that the metabolic activity of the cells slowed to a negligible rate, thus preventing product formation in the vial during sampling.

Determining the DCW proved problematic due to clumps of biofilm detaching from the main reactor volume and the outlet line, and entering the sample. DCW readings ranged from 2.0 g L^{-1} to 3.0 g L^{-1} for samples containing biofilm clumps, while clear samples, typically obtained at lower dilution rates, gave readings below 0.6 g L^{-1}. Variations in the DCW were addressed towards the end of the study where 24-h steady-state samples allowed for fluctuations to average out. However, 24-h samples were taken only for CSYE-medium runs.

Overall mass balances were performed to assess the accuracy of each sample. An elemental 'black box' stoichiometric model (Villadsen et al., 2011: 96–100) was used to perform the mass balances. The black box model solved for the stoichiometric amount of glucose required to achieve the experimental C_{SA}, C_{AA} and C_{FA}. This value was then compared with the experimentally obtained amount of glucose consumed. The percentage closure is calculated as the required stoichiometric amount of glucose divided by the experimental amount of glucose consumed. The DCW in the outlet was ignored due to the previously mentioned fluctuations. In calculating the amount of glucose consumed, the *effective* glucose concentration (C_{GLe}) was used which takes into account dilution of the reactor feed due to base and antifoam dosing. C_{GLe} was determined from Equation 3.7 where C_{GL0} is the glucose concentration in the medium, $(DV)_{exp}$ the experimentally determined volumetric flow rate, Q_{dose} the

calculated NaOH flow rate, and Q_{AF} the calculated antifoam flow rate. The numerator essentially reflects the experimental feed flow rate.

$$C_{GLe} = C_{GL0}\left(\frac{(DV)_{exp}/60 - Q_{dose} - Q_{AF}}{(DV)_{exp}/60}\right) \quad \textbf{3.7}$$

For the CSYE-medium runs, the mass balances closed to 94% on average with a standard deviation (σ) of 3.5%, which suggests that more glucose was consumed than was required to account for the metabolite production. The additional glucose is probably used in biomass synthesis as the 24-h samples with low DCWs closed to 98% on average (σ = 3.3%). The mass balances of the YE-medium runs without $Na_2S{\cdot}9H_2O$ closed to 87% on average (σ = 2.5%), and those with $Na_2S{\cdot}9H_2O$ closed to 92% (σ = 2.7%), suggesting that more biomass is produced when $Na_2S{\cdot}9H_2O$ is absent which causes slightly aerobic conditions. Furthermore, higher DCWs were observed for runs without $Na_2S{\cdot}9H_2O$.

3.8. Selection of the independent variable

Biofilm formation was unavoidable from the onset of all fermentations. It was also noted that a specific dilution rate was not associated with a specific consumption of glucose, hinting that the active biomass content in the reactor (X_{tot}) was dependent on the operation history of the fermentation, characterised by periods of growth, degradation and disintegration, and periods of apparent stability.

Since volumetric productivity cannot be related to dilution rate, X_{tot} should be used as the basis for the bioreactor design equation, where the biomass residence time (X_{tot}/Q) will be the true independent variable. X_{tot} is difficult to determine and requires termination of the fermentation; assumptions with

regard to the active fraction of biomass need to be made. The rate function will relate the glucose consumption to X_{tot}/Q; glucose consumption will increase with X_{tot}/Q. Accordingly, the glucose consumption was used as a relative indicator of X_{tot}/Q and used as the independent variable in the results reported below.

3.9. CO_2 flow rates

To determine the optimal feed flow rate of CO_2 to the reactor, the rate at which the pH of distilled water in the reactor decreased was monitored at different CO_2 flow rates and recycle pump flow rates. Normalised pH was used in order to account for slight variations in the starting pH of each test, thereby establishing a common starting point. The range of flow rates that resulted in the pH stabilising (i.e. CO_2 concentration reaching equilibrium) the fastest was selected as the operating range for the CO_2 flow rate. From Figure 3.4 it can be seen that a flow rate between 5% vvm and 10% vvm resulted in the most rapid approach to equilibrium, with 10% vvm being optimal.

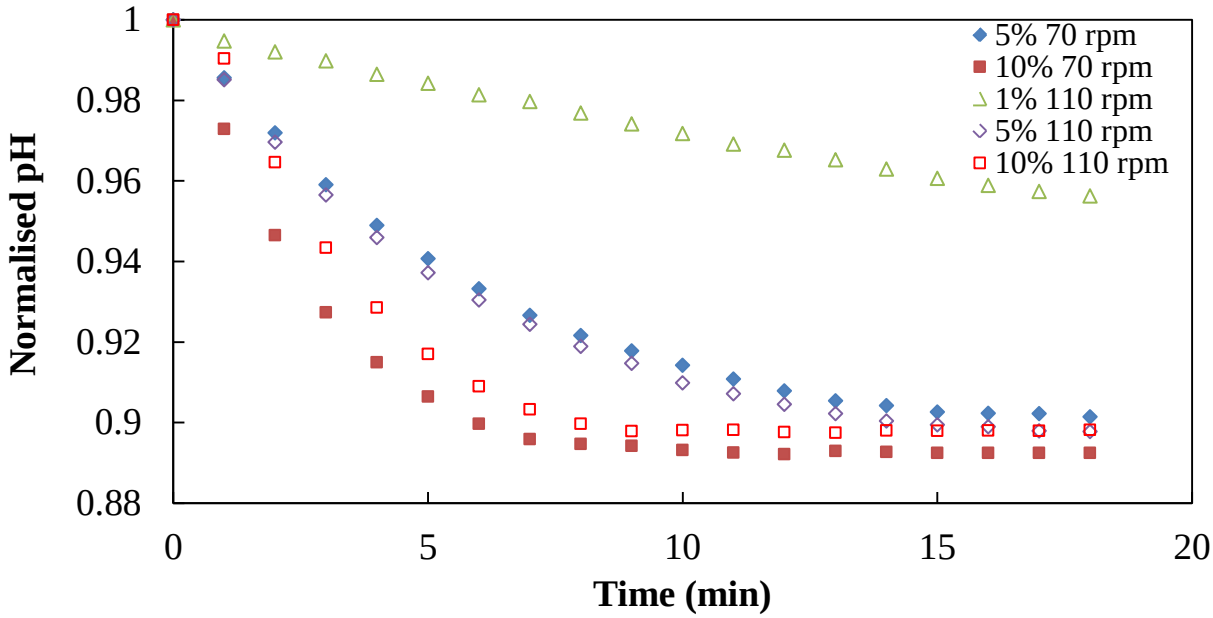

***Figure 3.4**: Normalised pH profiles (pH at time t divided by initial pH) over time for different CO_2 flow rates (% vvm) and different recycle pump speeds using Reactor B. CO_2 flow commenced at t = 0 min.*

In addition to the water-based tests above, CO_2 tests were performed online during certain YE-medium fermentations, and saturation checks were done during CSYE-medium runs. The saturation checks were performed by increasing the CO_2 flow rate and observing whether the time-averaged NaOH dosing profile increased, as this would indicate an increase in the medium acidity due to more CO_2 dissolving and/or an increase in SA production. From these checks it was determined that a flow rate between 2.8% vvm and 10% vvm is sufficient, depending on the productivity of the reactor and the flux distribution. If there is a substantial amount of biomass in the reactor, the productivity is higher and thus a higher CO_2 flow rate is required.

3.10. Reactor aspects

Control and transients

The variables and parameters of the reactor were monitored and controlled using a LabView program as outlined in Section 3.5. From Figure 3.5 (a & b) and Figure 3.6 (a & b) it can be seen that the temperature was controlled to within a degree of set-point (37 °C) and the pH was maintained to within 0.02 pH of set-point, with occasional overshoots. An example of the system achieving pseudo-steady state, during which the 24-h samples were taken, is illustrated by Figure 3.5 (c) where the time-averaged dosing profile of NaOH showed minor fluctuations (σ = 1.5%) over a 48-hour period.

A situation in which the system failed to achieve steady state due to biofilm instability and the need to transfer new medium is illustrated by Figure 3.6. When the fermentation medium was nearing depletion, it was necessary to decrease the dilution rate to prevent the reactor from entering a batch mode. This is usually prevented by preparing fresh medium in advance. However, problems in medium preparation were encountered and due to the high productivities that were occurring, the dilution rate was maintained.

Once the dilution rate had been decreased (Line A, Figure 3.6 (c)), the time-averaged dosing fraction showed a decreasing profile as the productivity of the reactor declined. The system then started to approach steady state at the new dilution rate, as seen by the gradual stabilisation of the dosing fraction. However, steady state was not achieved as the biofilm detached and disintegrated (Line B, Figure 3.6 (c)), leading to a linearly decreasing dosing profile. It was expected that the dosing profile would decrease in this fashion

since the amount of active biomass in the reactor decreased as the detached biofilm exited the system.

At the instant of biofilm detachment, the temperature (Figure 3.6 (a)) and pH (Figure 3.6 (b)) spiked, reflecting a momentary change in the composition of the fluid in the recycle line.

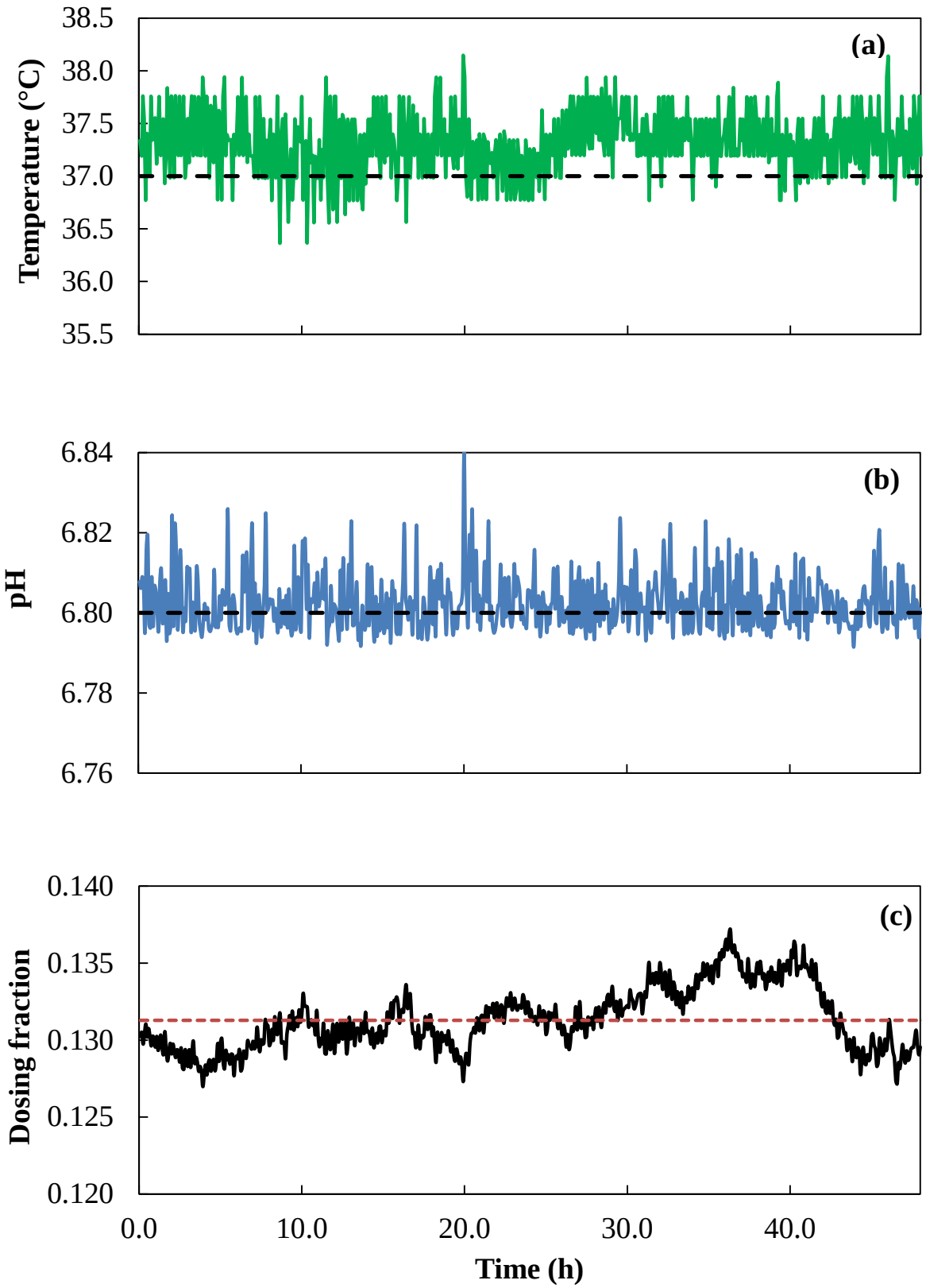

***Figure 3.5**: (a) Temperature, (b) pH, and (c) dosing profiles for a 48-h period (Reactor B) during which the 24-h samples were taken. Broken lines (a & b) indicate set-point values (T = 37.0 °C, pH = 6.80) and the average dosing fraction (c).*

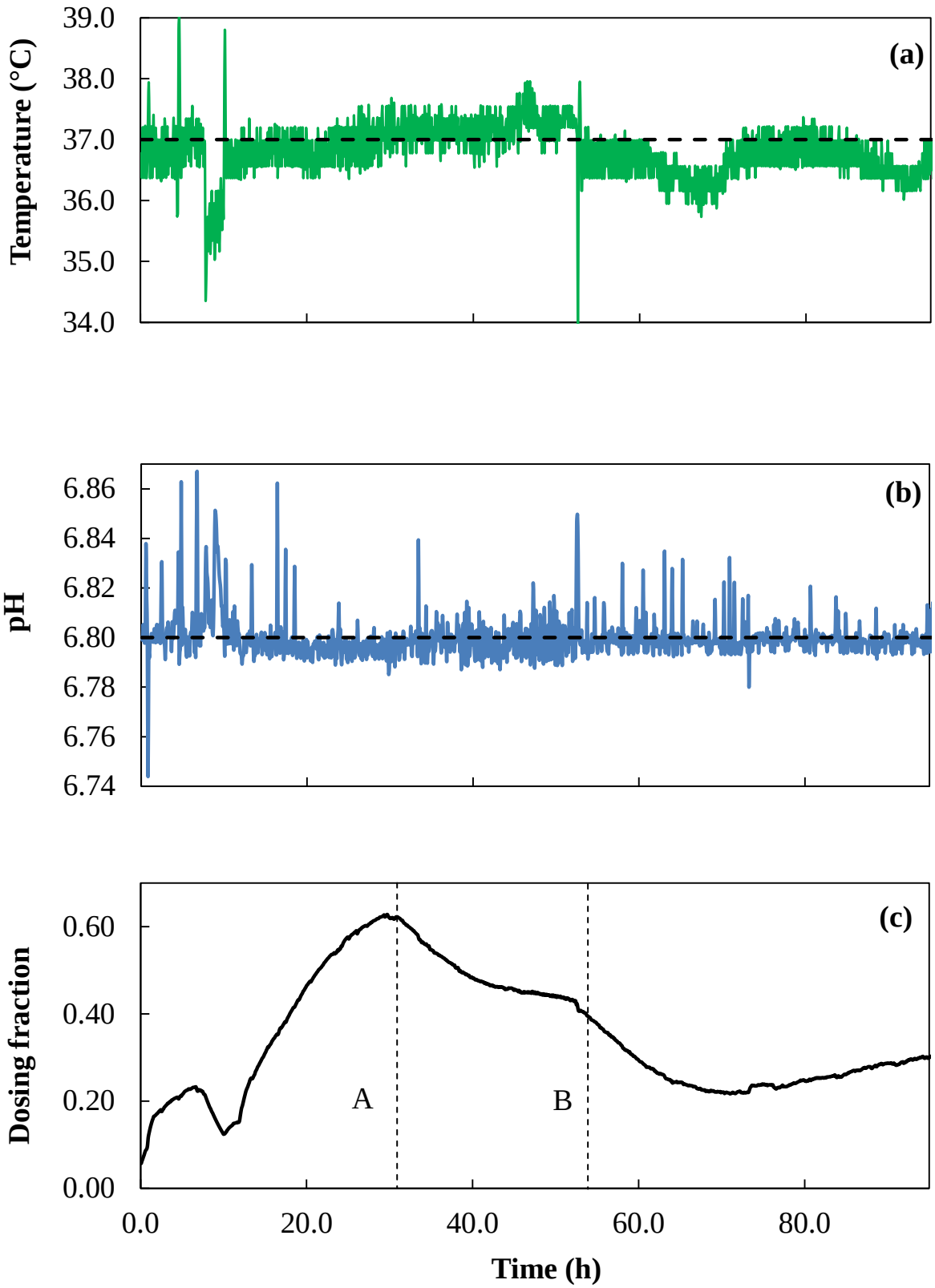

***Figure 3.6**: (a) Temperature, (b) pH, and (c) dosing profiles for a CSYE-medium run (Reactor B) in which biofilm instability was encountered. Horizontal broken lines indicate set-points.*

Biofilm appearance

Biofilm occurred in various forms and morphologies throughout this study. The structure of the biofilm seems to be a function of: (i) the surface to which it is attached; (ii) the extent of contact with the fermentation medium; (iii) the history of the fermentation; and (iv) the composition of the fermentation medium. Since this study was not an investigation into the structure of biofilm, only a few representative examples of the biofilm appearance are provided.

Figure 3.7 (c) shows the thin film of biofilm that occurred on the glass surface of Reactor A during fermentations with YE-medium. A similar type of biofilm was observed in Reactor B (Figure 3.8 (a)). The biofilm consisted of small wisp-like strands that collectively formed a thin layer on the surface of the glass. Such a structure appeared to have good mass transfer and good stability. Figures 3.7 (a) and (b) show the reactor before inoculation and without cell attachment respectively. The biofilm growth on the surface of the reactor was extensive since no resemblance to either Figure 3.7 (a) or Figure 3.7 (b) could be observed in Figure 3.7 (c). The white biofilm (Figure 3.7 (c)) developed from YE-medium, whereas the browner biofilm (Figure 3.8 (a)) grew on CSYE-medium.

In the empty headspace of Reactor B, biofilm with a thick, viscous texture tended to form (Figures 3.8 (a), (b) & (c)) and it had a darker complexion than the biofilm within the liquid-filled sections of the reactor. Biofilm in the headspace formed when foam was present, or when foam had been present in the headspace. The biofilm tended to form a continuous band along the inner circumference of the reactor above the surface of the liquid (Figure 3.8 (c)).

***Figure 3.7**: Images of Reactor A during various stages of fermentation: (a) before inoculation, (b) during growth but without biofilm formation, and (c) established biofilm on the reactor body (no packing)*

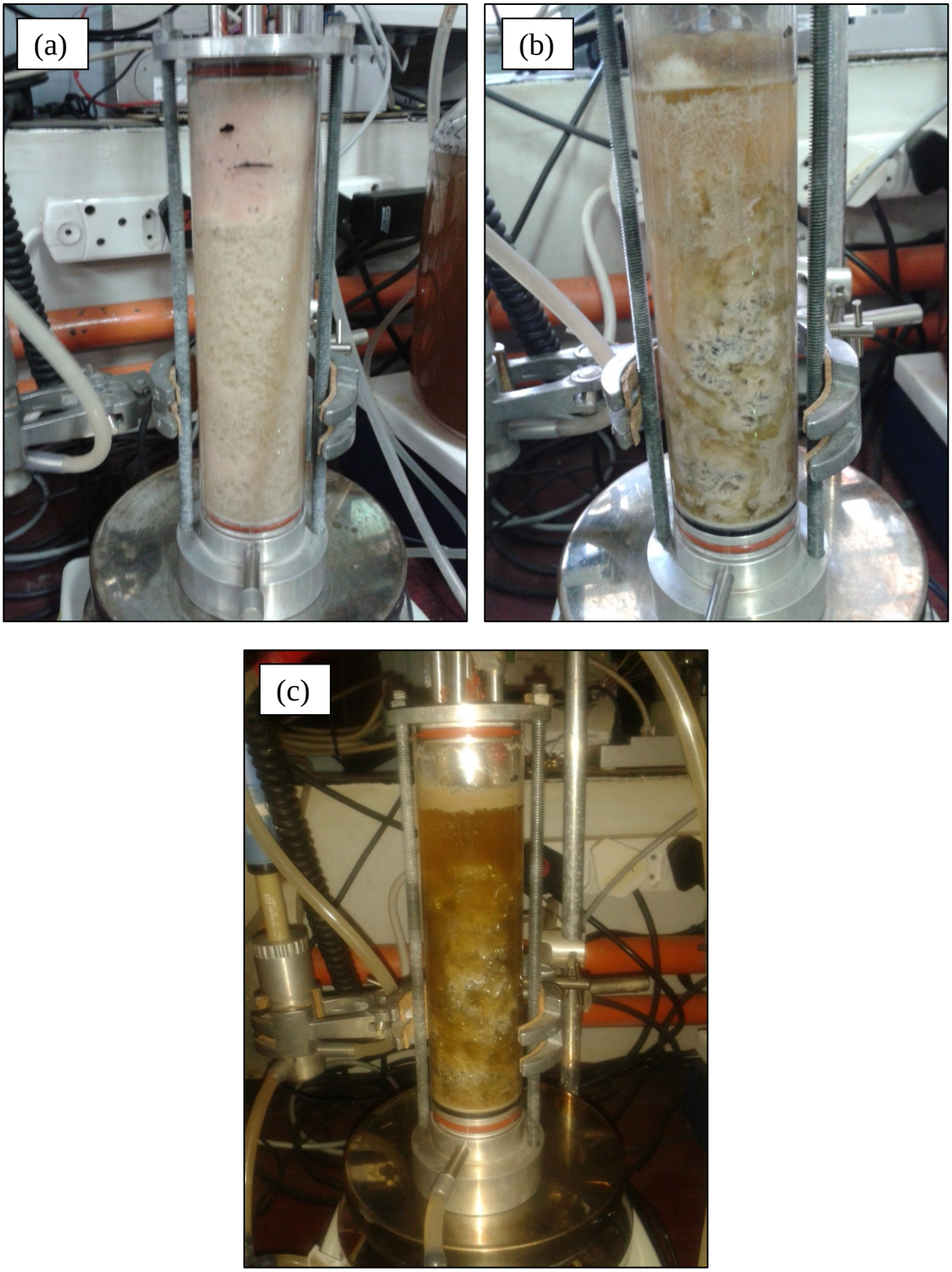

Figure 3.8: *Images of Reactor B during various stages of fermentation: (a) established biofilm on the reactor body (no packing), (b) biofilm on the reactor body and the stainless-steel packing, and (c) biofilm in the headspace of the reactor*

4. Results and Discussion

4.1. CSYE-medium fermentations

In the CSYE-medium fermentations (CSL and YE in feed), succinic acid concentration (C_{SA}) and acetic acid concentration (C_{AA}) increased with increasing glucose consumption. C_{SA} increased continuously at an increasing rate and C_{AA} increased at a diminishing rate, approaching a constant value at high values of glucose consumed (Figure 4.1). The concentration of formic acid (C_{FA}) increased up to 20 g L^{-1} glucose consumed and showed a steadily decreasing trend towards zero with increasing glucose consumption. Ethanol concentrations were found to be negligible. The highest values achieved for C_{SA}, SA productivity (q_{SA}) and glucose conversion (γ) – summarised in Table 4.1 – all exceed the highest values reported in the literature (Table 2.1) for continuous fermentations with *A. succinogenes*. Note that substrate limitation did not occur for runs where the glucose feed concentration was 60 g L^{-1}.

***Table 4.1**: Summary of the highest values achieved for the CSYE-medium fermentations. Values in bold signify maxima. All CSYE-medium data are given in Appendix A.*

C_{GLe}* (g L^{-1})	C_{SA} (g L^{-1})	q_{SA} (g L^{-1} h^{-1})	γ	D (h^{-1})	ΔGL (g L^{-1})
62.9	**48.5**	3.4	0.92	0.07	57.9
29.1	21.9	2.4	**0.99**	0.11	29.0
65.9	17.5	**9.4**	0.35	0.54	23.2

* *Effective glucose concentration in feed – see Equation 3.7 for calculation thereof.*

In the event of constant metabolic flux across all values of glucose consumed, the acid concentrations should all increase linearly, with an intersection through the origin (i.e. constant yields on glucose). Since Figure 4.1 indicates that the acid concentrations did not follow a linear profile, it is clear that the steady-state metabolic flux of *A. succinogenes* varied with increasing glucose consumption. Furthermore, it is evident that the flux shifted in favour of SA production at increasing values of glucose consumed. The shift in metabolic flux is further evidenced by variations in the relative ratios of the products. This is illustrated in Figure 4.2 which shows that Y_{AASA} increased and Y_{AAFA} decreased with increasing glucose consumption. The appreciable increase in Y_{AASA} exemplifies the flux shifting in favour of SA production.

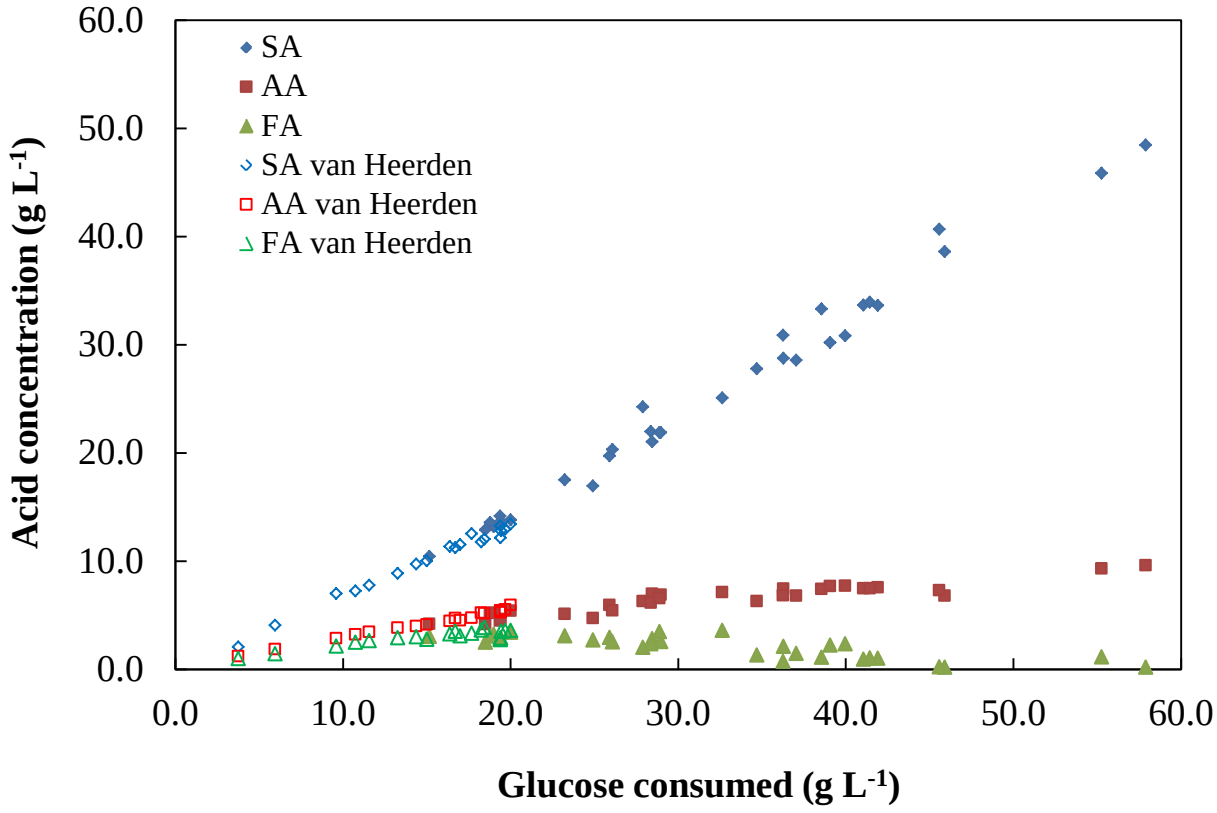

Figure 4.1: *Product profiles for CSYE-medium runs. The open markers, used to extend the data to low values of glucose consumed, represent data from Van Heerden & Nicol (2013a). Each data point represents a sample of the bioreactor at pseudo-steady state.*

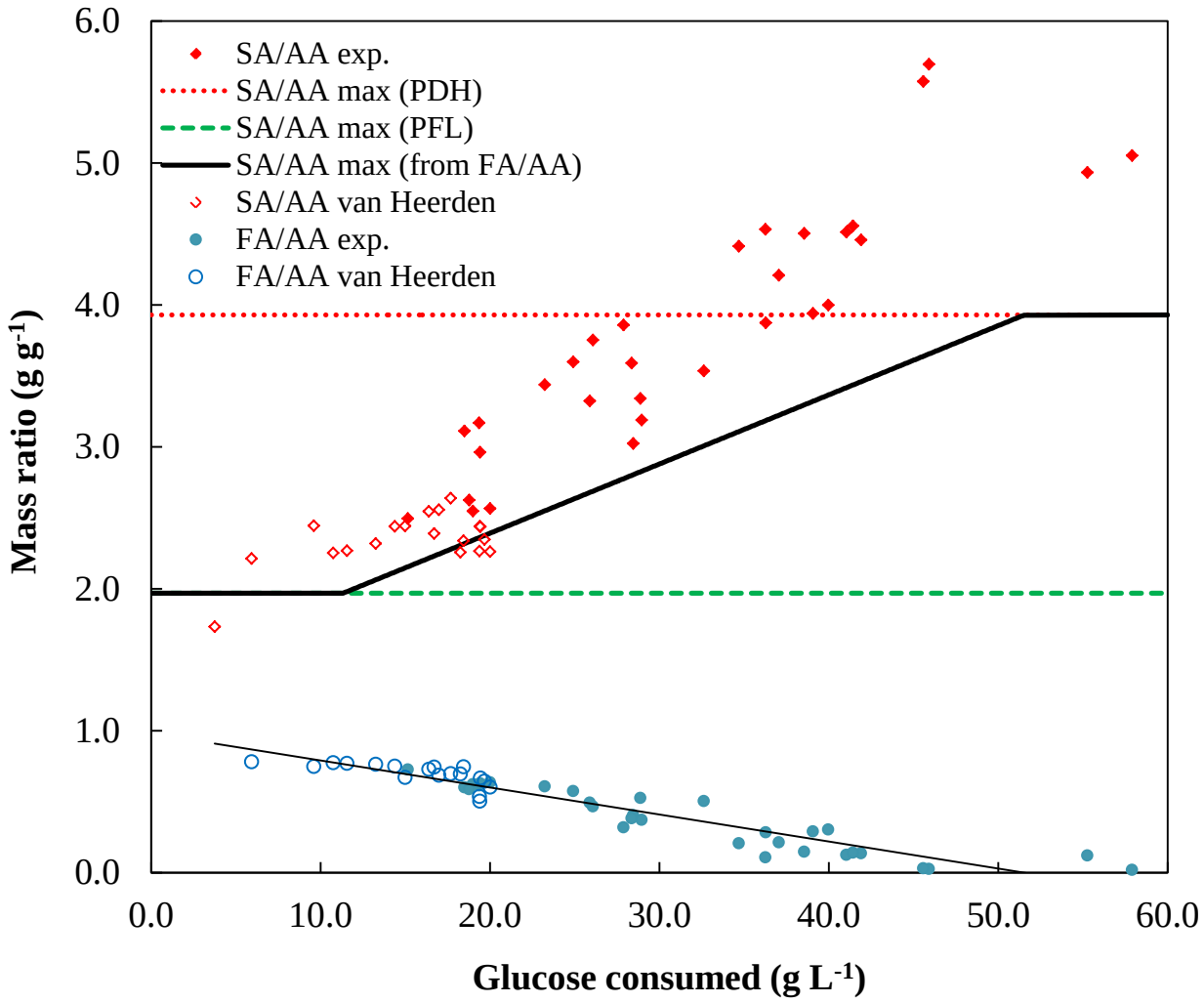

***Figure 4.2**: Product ratios for the CSYE-medium runs. The broken lines at 3.93 g g^{-1} and 1.97 g g^{-1} indicate the maximum Y_{AASA}, depending on the pyruvate oxidation route. The solid line between the two broken lines represents the maximum Y_{AASA} based on the corresponding Y_{AAFA} value (determined from the trend line through the Y_{AAFA} data points and a carbon and redox balance). The open markers are selected data from Van Heerden & Nicol (2013a) and were used to extend the profiles to lower values of glucose consumed.*

4.2. Theoretical analysis of metabolic flux variation

Metabolic pathways in A. succinogenes

Optimising carbon flux to SA is essential for the bioproduction of SA to be commercially viable. Wild-type *A. succinogenes* 130Z produces SA via the phosphoenolpyruvate carboxykinase pathway (Section 2.2.2) and the reductive branch of the TCA cycle (C_4 pathway, Figure 4.3). As this is a reductive pathway, it results in a net consumption of NADH. Acetic acid and formic acid are produced via pyruvate oxidation (C_3 pathway), which serves as the oxidative complement to the C_4 pathway, and completes the metabolism of carbon and satisfies the redox balance. Flux to SA in *A. succinogenes* is therefore constrained owing to the need to satisfy the redox balance.

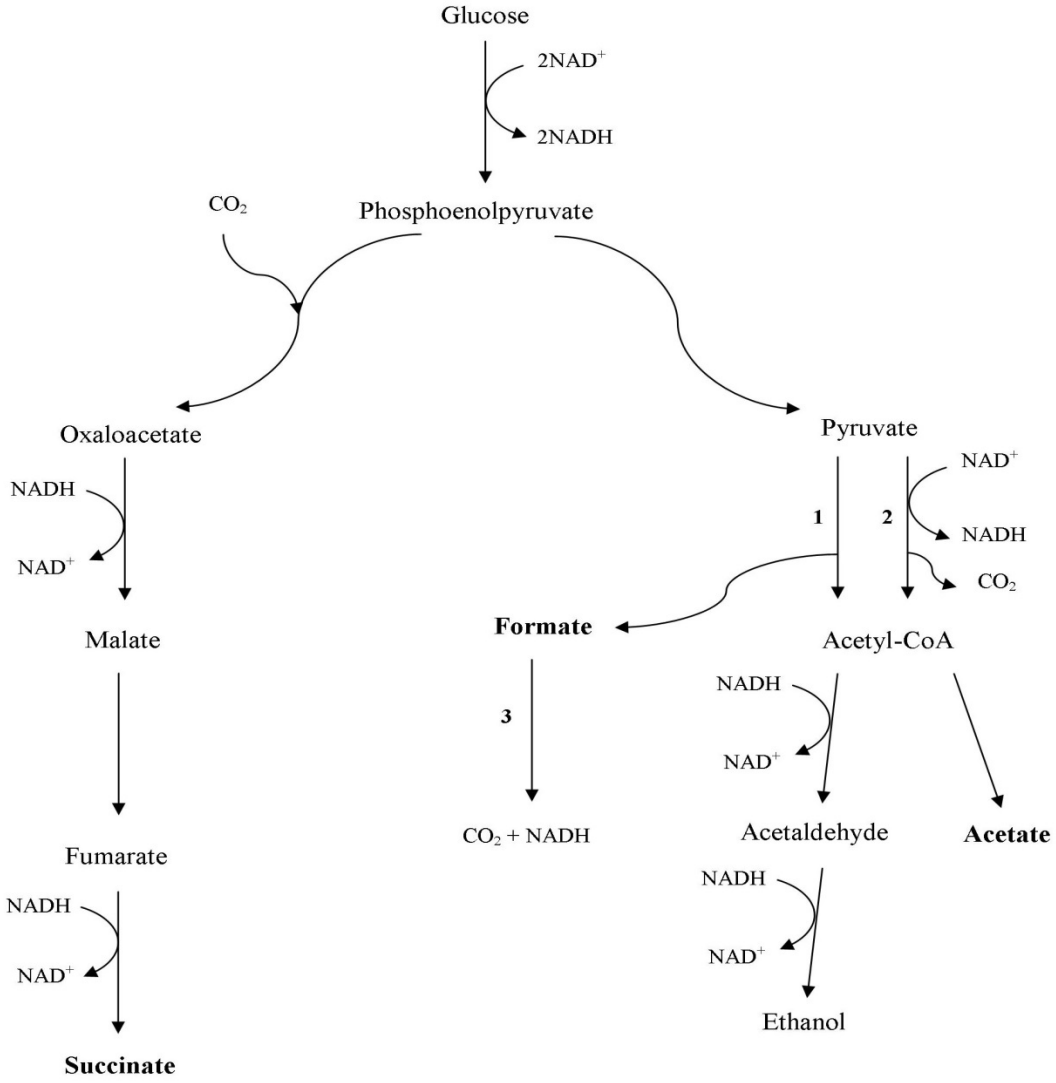

***Figure 4.3**: Simplified metabolic network of A. succinogenes showing the pathways leading to its major metabolites and redox flow (based on McKinlay et al. (2007)). The relevant enzymes are (1) pyruvate-formate lyase, (2) pyruvate dehydrogenase and (3) formate dehydrogenase. ATP flow is excluded. (Figure 2.2 repeated)*

In *A. succinogenes*, the metabolism of pyruvate can occur via two pathways, namely the pyruvate-formate lyase (PFL) pathway or the pyruvate dehydrogenase (PDH) pathway (Section 2.2.2). In the PFL route, Y_{AAFA} is 1.0 mol mol^{-1} since the Ac-CoA formed from pyruvate is converted into a single AA molecule (Figure 4.3). Alternatively, if the PDH pathway is active, no FA is produced but instead CO_2 and NADH, hence Y_{AAFA} is zero and additional

reducing power is generated. Similarly, if the PFL pathway is active in conjunction with formate dehydrogenase (FDH), CO_2 and NADH are produced in the breakdown of FA by FDH, resulting in Y_{AAFA} becoming zero. The following reactions occur when pyruvate is converted exclusively by PFL:

$$GL + 2CO_2 + 2NADH \rightarrow 2SA \quad \textbf{4.1}$$

$$GL \rightarrow 2AA + 2FA + 2NADH \quad \textbf{4.2}$$

Equation 4.1 represents SA production, and Equation 4.2 represents AA and FA production. Combining Equations 4.1 and 4.2 yields the net, redox-balanced Equation 4.3:

$$GL + CO_2 \rightarrow SA + AA + FA \quad \textbf{4.3}$$

Equation 4.3 reflects that the maximum value for Y_{AASA} is 1.0 mol mol^{-1} = 1.97 g g^{-1} and the maximum Y_{GLSA} is 0.66 g g^{-1}, provided no biomass is formed, i.e. if all the carbon is converted to metabolites. Alternatively, if the conversion of pyruvate proceeds via the PDH pathway, the following reactions occur:

$$2GL + 4CO_2 + 4NADH \rightarrow 4SA \quad \textbf{4.4}$$

$$GL \rightarrow 2AA + 2CO_2 + 4NADH \quad \textbf{4.5}$$

Equation 4.4 is simply Equation 4.1 multiplied by two to satisfy overall redox requirements and Equation 4.5 represents AA production. Similar to the above, combining Equations 4.4 and 4.5 yields the net, redox-balanced Equation 4.6.

$$3GL + 4CO_2 \rightarrow 4SA + 2AA \quad \textbf{4.6}$$

It follows from Equation 4.6 that, in the absence of biomass formation, the maximum value for Y_{AASA} is 2.0 mol mol^{-1} = 3.93 g g^{-1} and the maximum for Y_{GLSA} is 0.87 g g^{-1}. If FA is produced via the PFL route, it is possible for it to be converted to CO_2 and NADH by FDH, which also gives a maximum value of 3.93 g g^{-1} for Y_{AASA}, with no biomass formation. If biomass is synthesised, a portion of glucose will be channelled to anabolic pathways and the redox balance will be affected, resulting in maximum yields less than those given above. The above maxima are based on the central metabolism of *A. succinogenes* and pertain specifically to the pathways depicted in Figure 4.3.

Product ratios

Despite these limitations on the product ratios, Y_{AASA} in this study consistently increased above values of 3.93 g g^{-1} at glucose consumptions greater than 30 g L^{-1} (Figure 4.2), and showed an upward trend which indicated a shift in the metabolic flux distribution. The highest Y_{AASA} value obtained in this study was 5.7 g g^{-1} at a glucose consumption of 46 g L^{-1}, which is the highest value obtained for continuous fermentations with *A. succinogenes* to date (Table 2.1), the highest Y_{AASA} value found in the literature being 2.8 g g^{-1} (Kim et al., 2009). By contrast, batch studies on *A. succinogenes* (Table 2.2) report Y_{AASA} values above the theoretical limit derived above. The highest value obtained in a batch reactor is 15.3 g g^{-1} (Xi et al., 2012) using a chemically defined medium and strain NJ113. It is desirable to achieve the same metabolic flux distribution (i.e. product ratio) in a continuous fermentation as this would improve overall reactor performance.

Considering flux at the pyruvate node, Y_{AAFA} decreased towards zero with increasing glucose consumption (Figure 4.2), which suggests an increase in either PDH or FDH activity. The redox balance dictates an increase in Y_{AASA}

following a decrease in Y_{AAFA}, as indicated by the solid black linear profile in Figure 4.2. The solid black line was generated by fitting a linear trend line to the experimental Y_{AAFA} data in Figure 4.2 and solving for the corresponding Y_{AASA} value using carbon and redox balances. The experimental Y_{AASA} values exceeded the predicted values, implying that an increase in PDH or FDH activity is not the only contribution to the increase in Y_{AASA} and that additional reducing power is present.

Yield on glucose

The shift in metabolic flux towards SA formation is further evidenced by the increase in Y_{GLSA} with increasing glucose consumption (Figure 4.4). The highest Y_{GLSA} achieved was 0.91 g g^{-1} with the yields on glucose exceeding 0.68 g g^{-1} across all values of glucose consumed and all fermentation conditions. Five Y_{GLSA} values exceeded the theoretical limit of 0.87 g g^{-1} based on the metabolic network in Figure 2.2, which dovetails with Y_{AASA} exceeding its theoretical limit. However, it is expected that Y_{GLSA} would be greater than or equal to 0.87 g g^{-1} for all data points where Y_{AASA} exceeded the theoretical maximum. The deviation can be explained by the incomplete closure of the mass balances discussed in Section 3.7, where a portion of glucose is channelled into biomass synthesis, thereby reducing the total amount available for metabolite production. To date, this is the highest yield on glucose achieved for a continuous fermentation with *A. succinogenes* (Table 2.1). Compared with batch fermentations (Table 2.2), only Xi et al. (2012) report a higher yield of 0.94 g g^{-1} using strain NJ113.

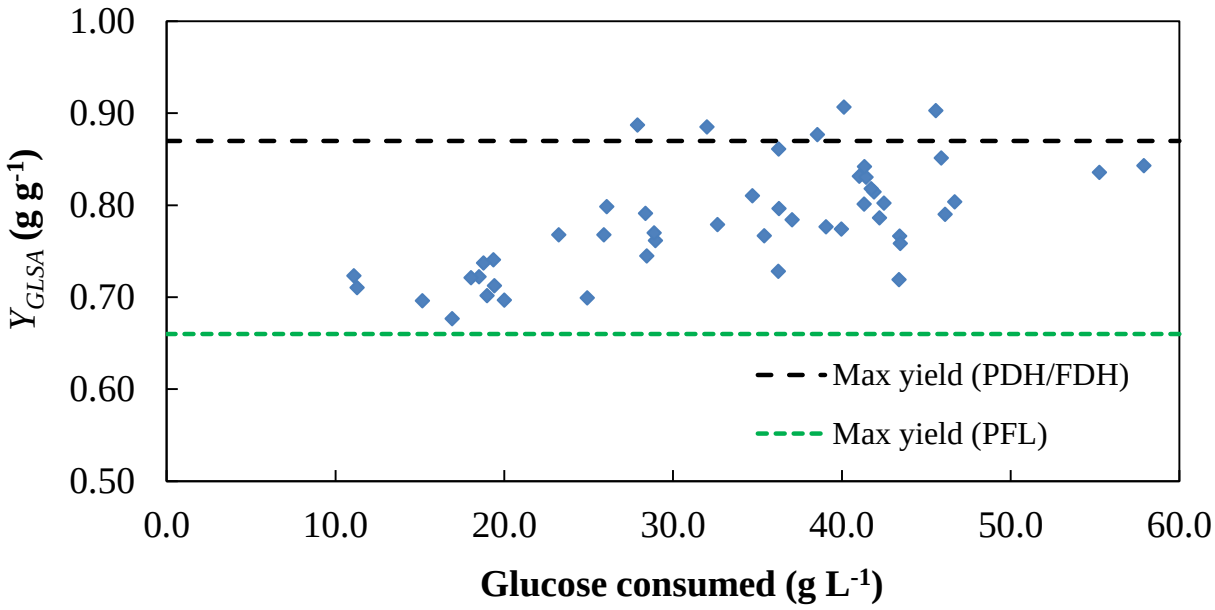

***Figure 4.4**: Yield of succinic acid on glucose for the CSYE-medium runs. The maximum yield for the PDH/FDH pathway is 0.87 g g^{-1} and that for the PFL pathway is 0.66 g g^{-1}.*

Reducing power from biomass

Biomass formation can be associated with the net formation of NADPH despite biomass being more reduced than glucose. This is due to the fact that CO_2 is released during biomass formation as reflected by the following redox and carbon balanced equation (Villadsen, Nielsen & Lidén, 2011: 159):

$$(1+\alpha)CH_2O \rightarrow X + \alpha CO_2 + \frac{1}{2}[4(1+\alpha) - \kappa_X]NADH \qquad \textbf{4.7}$$

In Equation 4.7 the loss of carbon as CO_2 is represented by the coefficient α and the reduction level of biomass (X) is given by κ_x. In addition, the NADPH associated with biomass production is represented as NADH. In this study the standard composition of biomass was used ($CH_{1.8}O_{0.5}N_{0.2}$, Villadsen et al., 2011: 74) which results in a κ_x value of 4.2 if redox levels of 4, 1, -2 and -3 are used for C, H, O and N respectively. Using a value of 0.1 for α, which lies between the guideline values of 0.08 and 0.14 (Villadsen, Nielsen & Lidén, 2011: 159),

results in the coefficient of NADH being equal to 0.1. Therefore, it is possible for NADH to be released in biomass formation. It could, therefore, be possible for biomass production to serve as the source of the additional NADH. McKinlay et al. (2007) determined that *A. succinogenes* possesses a transhydrogenase (an enzyme that can be used to convert NADPH to NADH), although they suggest that in *A. succinogenes* the enzyme converts excess NADH to NADPH. It must, therefore, be determined whether the reducing power generated from biomass accounts for the additional redox required to close the redox balance.

In this regard, it is useful to analyse the additional or *excess* NADH required to satisfy the redox balance at high Y_{AASA} values as a function of glucose consumption. The *excess* NADH can be expressed as the moles of NADH generated beyond the pathway in Figure 2.2, per mole of glucose consumed (i.e. mol mol^{-1}). All components are expressed on a carbon-mole (C-mol) basis. This is useful to account for the total flow of carbon through the metabolic network, especially when biomass is considered.

The 24-hour sample at a glucose consumption of 41.4 g L^{-1} resulted in a DCW of 0.2 g L^{-1}. Taking the standard molecular composition of biomass as $CH_{1.8}O_{0.5}N_{0.2}$ and the metabolic network in Figure 2.2, the NADH formed via the generation of biomass (0.003 mol mol^{-1}), glycolysis (1.99 mol mol^{-1}) and the PDH/FDH pathway (0.214 mol mol^{-1}) is only 87% of that required to produce 34.5 g L^{-1} SA. The *excess* NADH is therefore 0.336 mol mol^{-1}. Similar results were obtained for the other 24-hour samples. This implies that the additional reducing power generated from biomass production and the PDH/FDH pathway collectively does not account for the extra NADH required to satisfy the high Y_{AASA} values.

Reducing power in medium

Unidentified sources of reducing power that can be utilised by *A. succinogenes* for reduction reactions or compounds that can be oxidised by the organism may be present in the fermentation medium. One such possibility is the consumption of lactic acid (LA), as there are significant amounts of lactic acid present in corn steep liquor and *A. succinogenes* possesses a lactate dehydrogenase capable of lactate oxidation (McKinlay et al., 2010). In this study it was found that the feed had an average LA concentration of 0.46 g L^{-1}. The average change in LA concentration during the fermentations was -12.7%, with a standard deviation of 15.2%. Despite the average decrease in LA concentration, the possible contribution from LA to the *excess* NADH is only 0.7% on average. In other words, if LA was consumed by *A. succinogenes*, the associated NADH generated would only account for 0.7% of the extra NADH, on average. Therefore, LA does not serve as the source of the additional reducing power. Furthermore, no other compounds were detected that were initially present in the feed and consumed during fermentations. Corona-González et al. (2008) and Xi et al. (2012) report Y_{AASA} values greater than the theoretical maximum in batch runs using yeast extract and a defined medium respectively. This suggests that the shift in metabolic flux is attainable without corn steep liquor. However, the above arguments do not fully eliminate the medium as the possible source of the additional NADH.

To further explore this possibility, the yield profiles given in Figure 4.2 were fitted with empirical least squares fits, which were used to determine the *excess* NADH as a function of glucose consumption (Figure 4.5) based on metabolic flux balancing. It is clear that the additional reducing power increases as the glucose consumption (or X_{tot}/Q) increases. If a limited amount of reducing power was present in the fermentation medium and it was completely

consumed, the trend in Figure 4.5 would be reversed. That is to say, if a finite amount of reducing power was available and consumed by the organism, the graph should follow a hyperbolic curve as the NADH source would be stoichiometrically limited. Lower glucose consumption would then be associated with a higher fraction of *free* reducing power. It is also possible that the consumption of potential NADH in the medium is rate limited. In this case, the lower glucose depletion rates at higher glucose consumptions will result in a larger fraction of *excess* NADH per glucose consumed, as reflected in Figure 4.5. Accordingly, the medium serving as the source of the *excess* NADH remains a possibility.

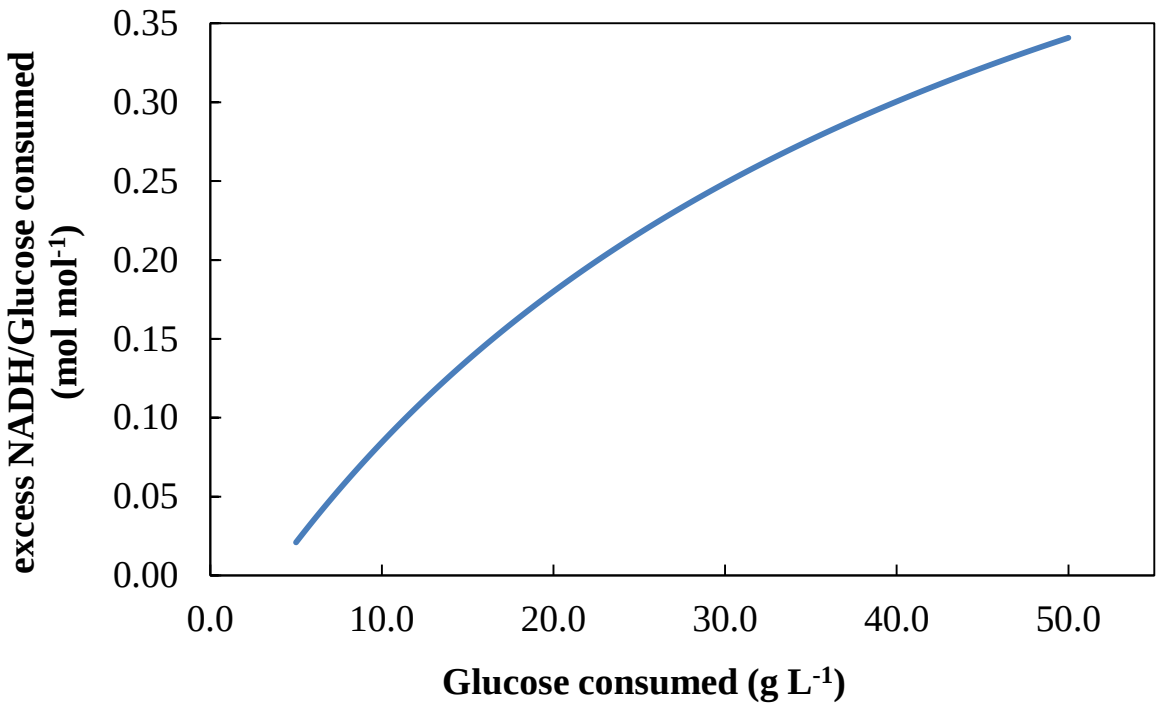

***Figure 4.5**: Excess NADH required to produce the corresponding C_{SA} at a given value of glucose consumed, relative to NADH generated by the central metabolic network of A. succinogenes*

Reducing power from a metabolic process

It is also possible that a metabolic process delivers the *excess* NADH or NADPH. The oxidative branch of the TCA cycle and the glyoxylate shunt are able to generate additional NADH independently thereby increasing C_4 pathway flux and the maximum Y_{GLSA} to 1.12 g g^{-1} without biomass and by-product formation, as discussed in van Heerden & Nicol (2013b). However, *A. succinogenes* lacks the TCA cycle enzymes citrate synthase and isocitrate dehydrogenase (McKinlay, Zeikus & Vieille, 2005) as well as a functional glyoxylate shunt (McKinlay et al., 2007). Therefore, these pathways can be ruled out as the sources of the additional NADH. Rühl, Le Coq, Aymerich & Sauer (2012) demonstrated that resting, non-growing *Bacillus subtilis* cells show sustained metabolic activity without cell growth, which leads to an apparent catabolic overproduction of NADPH (via the pentose phosphate pathway) that is converted to NADH by transhydrogenase. A similar mechanism could occur in *A. succinogenes* as it does possess transhydrogenase, as mentioned above. Such a mechanism can explain the source of additional reducing power observed in this study. If the additional reducing power is generated from a metabolic process, it is necessary to elucidate the process and determine the conditions under which it is most active.

Maintenance

It is known that the growth of *A. succinogenes* is inhibited by the presence of organic acids (Corona-González et al., 2008; Corona-Gonzalez, Bories, González-Alvarez, Snell-Castro, Toriz-González & Pelayo-Ortiz, 2010; Urbance et al., 2004; Lin et al., 2008). Despite the growth inhibition due to high acid concentrations, the results from batch fermentations with *A. succinogenes* suggest that organic acids continue to be produced after the termination of cell

growth (Corona-González et al., 2008; Lin et al., 2008; Liu, Zheng, Sun, Ni, Dong & Zhu, 2008; Xi et al., 2012, 2013), which tends to occur between 11 g L^{-1} and 28 g L^{-1} total acids concentration and between 8 g L^{-1} and 19 g L^{-1} succinate concentration, depending on the fermentation medium and conditions. These results suggest that *A. succinogenes* is capable of producing SA, AA and FA in a non-growth or maintenance state.

Furthermore, in certain batch fermentations with *A. succinogenes* (Corona-González et al., 2008; Liu et al., 2008; Xi et al., 2013, 2012), the data suggest that the metabolic flux distribution shifted in favour of SA production at the point at which cell growth terminated. The shift in flux distribution is reflected by an increase in Y_{AASA} as the biomass (DCW) concentration decreased. In the present study, an average DCW of 0.2 g L^{-1} was obtained from three 24-h samples with an established biofilm present and the system at pseudo-steady state. During the sampling intervals Y_{AASA} was between 3.8 g g^{-1} and 4.5 g g^{-1}, with glucose consumption between 40 g L^{-1} and 44 g L^{-1}. By contrast, the DCWs in situations with less observed biofilm were higher (1.7 g L^{-1} to 2.4 g L^{-1}) and Y_{AASA} was between 2.6 g g^{-1} and 3.5 g g^{-1}, with glucose consumption between 19 g L^{-1} and 27 g L^{-1}. Although the absolute values of the DCWs are questionable (as discussed in Section 3.7), the differences in magnitude qualitatively suggest a difference in the behaviour of the bacteria. At high SA concentrations, the growth of biomass appears to decrease (i.e. there is a decrease in DCW in the reactor outlet), which implies that the cells have entered a maintenance or non-growth state as mentioned above. Furthermore, the accompanying increase in Y_{AASA} suggests that succinate production is favoured in this state.

The notion of *A. succinogenes* entering a maintenance state with a different metabolic flux distribution ties in with the work by Rühl et al. (2012), and it is

possible that the additional reducing power is generated by sustained activity of the pentose phosphate pathway. The presence of biofilm may play a role in increasing the variation in metabolic flux as biofilm can comprise cells expressing distinct metabolic pathways (Stewart & Franklin, 2008) and the maintenance state may therefore be more pronounced in sessile cells. Also, the higher Y_{AASA} values were obtained with the presence of an established biofilm.

Pyruvate node

As mentioned above, Y_{AAFA} was found to decrease from 0.77 g g^{-1} (equimolar amounts) to values approaching zero (Figure 4.2). Furthermore, Y_{AASA} tended to be greater than 1.97 g g^{-1} for all amounts of glucose consumed, which suggests that either the PDH pathway or the FDH pathway (after initial FA production via the PFL pathway), or both, is active and becomes increasingly so with increasing glucose consumption. Van der Werf et al. (1997) determined the specific activity of PDH, PFL and FDH in end-product formation in *A. succinogenes* to be less than 1, 390 and 12 nmol min^{-1} mg $protein^{-1}$ respectively. Moreover, in batch experiments with *A. succinogenes*, Xi et al. (2012) and Du, Lin, Koutinas, Wang, Dorado & Webb (2008) reported that C_{FA} increased up to a point, then decreased as the fermentation proceeded. The higher FDH activity and the decrease in C_{FA} with time in some batch fermentations provides evidence that the PFL-FDH pathway is probably the primary route of pyruvate metabolism.

4.3. YE-medium fermentations

Most of the data for the YE-medium fermentations were collected early in the study using Reactor A. Foaming problems and insufficient biofilm support resulted in overall stability problems in the reactor, making it difficult to attain steady state. Furthermore, as mentioned in Section 3.7, the mass balances for runs in Reactor A were poorer than those for Reactor B.

In the fermentations using YE-medium, the concentrations of all the products increased with increasing glucose consumption (Figure 4.6). As with the CSYE-medium fermentations, ethanol production was found to be negligible. In contrast to the CSYE-medium fermentations (Figure 4.1), C_{FA} did not fall to zero and C_{AA} did not flatten out with increasing glucose consumption. However, C_{AA} and C_{FA} increased at a decreasing rate at glucose consumptions greater than 30 g L^{-1}. Together with this, the value of Y_{AASA} was greater at glucose consumptions above 30 g L^{-1} (Figure 4.7), suggesting a shift in the metabolic flux distribution. Runs without $Na_2S{\cdot}9H_2O$ resulted in lower SA concentrations. Table 4.2 summarises the highest values achieved for C_{SA}, q_{SA} and glucose conversion for the YE-medium runs. While the maximum C_{SA} and q_{SA} values are significantly less than those for the CSYE-medium fermentations (Table 4.1), the maximum glucose conversion is within 10% of that achieved for the CSYE-medium fermentations. Interestingly, the highest C_{SA} attained in this study for YE-medium fermentations exceeded that for continuous fermentations in the literature that used YE- and CSL-based media (Table 2.1).

***Table 4.2**: Summary of the highest values achieved for the YE-medium fermentations. Values in bold signify maxima. All YE-medium data are given in Appendix B.*

C_{GLe}* (g L^{-1})	C_{SA} (g L^{-1})	q_{SA} (g L^{-1} h^{-1})	γ	D (h^{-1})	ΔGL (g L^{-1})
51.2	**29.5**	1.9	**0.90**	0.05	46.2
53.2	26.9	**3.1**	0.71	0.11	38.0

**Effective glucose concentration in feed–- see Equation 3.7 for calculation thereof.*

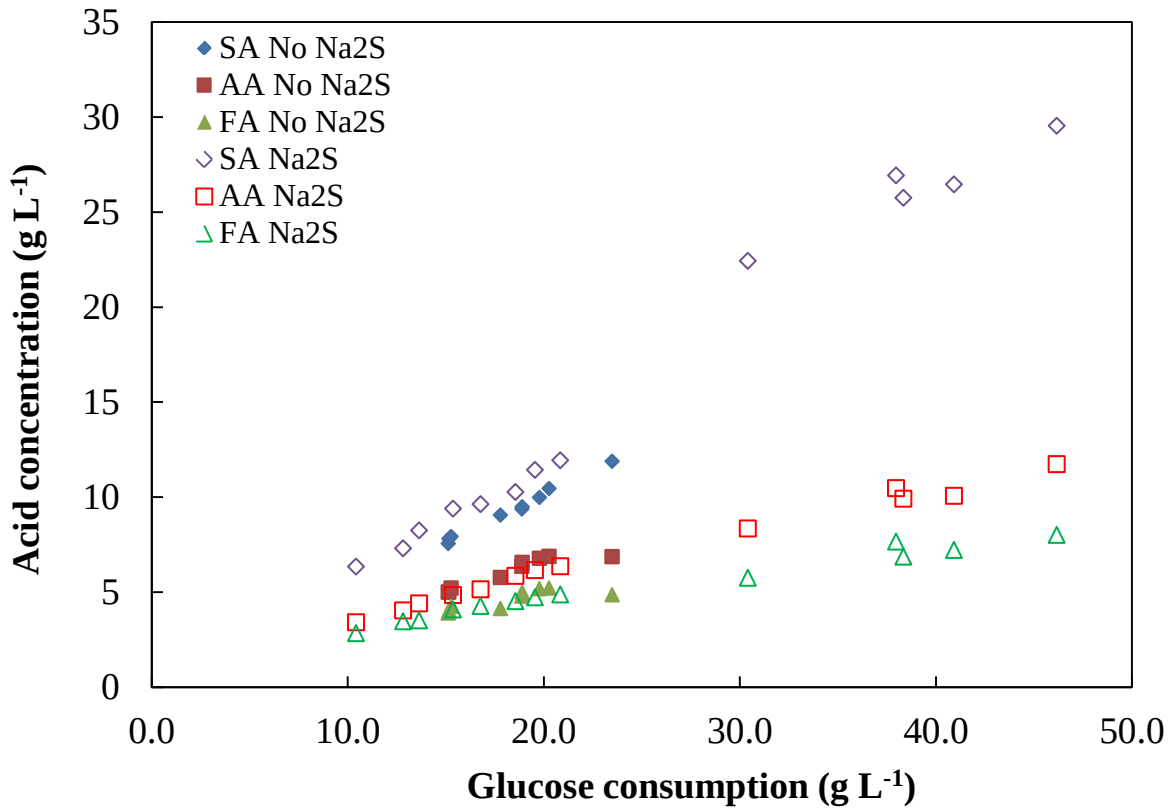

Figure 4.6: *Product profiles for YE-medium fermentations. Open markers represent runs with $Na_2S{\cdot}9H_2O$ present in the medium; closed markers represent runs where $Na_2S{\cdot}9H_2O$ was excluded from the medium.*

Product ratios

At glucose consumptions greater than 30 g L^{-1}, the values of Y_{AASA} obtained for the YE-medium runs (Figure 4.7) were greater than the theoretical maximum for purely PFL-based pyruvate conversion (1.97 g g^{-1}), but below the highest theoretical maximum (3.93 g g^{-1}) for the established metabolic network (Section 4.2). The results for glucose consumptions greater than 30 g L^{-1} were obtained with an established biofilm originally grown on CSYE-medium in the more stable Reactor B; CSYE-medium was replaced with YE-medium during the fermentation.

At lower glucose consumptions, Y_{AASA} was around 1.97 g g^{-1} in fermentations containing $Na_2S{\cdot}9H_2O$ and below 1.97 g g^{-1} in fermentations without $Na_2S{\cdot}9H_2O$ (Figure 4.7). Furthermore, introducing air to the system resulted in Y_{AASA} values below 1.97 g g^{-1} with a linearly increasing trend towards 1.97 g g^{-1}, with the Y_{AAFA} values remaining at around 0.77 g g^{-1}. The increase towards 1.97 g g^{-1} corresponds to a decrease in the partial pressure of oxygen in the system since the CO_2 flow rate was incrementally increased during the air experiments. Effectively, this means that a greater oxygen concentration (i.e. partial pressure) resulted in a lower Y_{AASA} value. From a redox perspective, it suggests that an alternative NADH sink is present since the C_4 pathway flux is lower. The DCWs for the aerated cases ranged between 2.4 g L^{-1} and 2.9 g L^{-1}, which is greater than those for the anaerobic cases (1.6 g L^{-1} to 2.2 g L^{-1}). The concomitant increase in biomass with a decrease in Y_{AASA} suggests that oxidative phosphorylation may be active since it is an NADH sink, requires O_2 and generates ATP which is used in biomass synthesis.

The highest Y_{AASA} achieved was 2.7 g g^{-1}, which compares well the 2.8 g g^{-1} achieved by Kim et al. (2009) who also used a YE-medium in a continuous

fermentation. However, Corona-González et al. (2008) achieved a Y_{AASA} of 5.2 g g^{-1} using YE-medium, although in a batch reactor, which suggests that *A. succinogenes* may have the potential to achieve greater C_4 pathway flux in a continuous fermentation with YE.

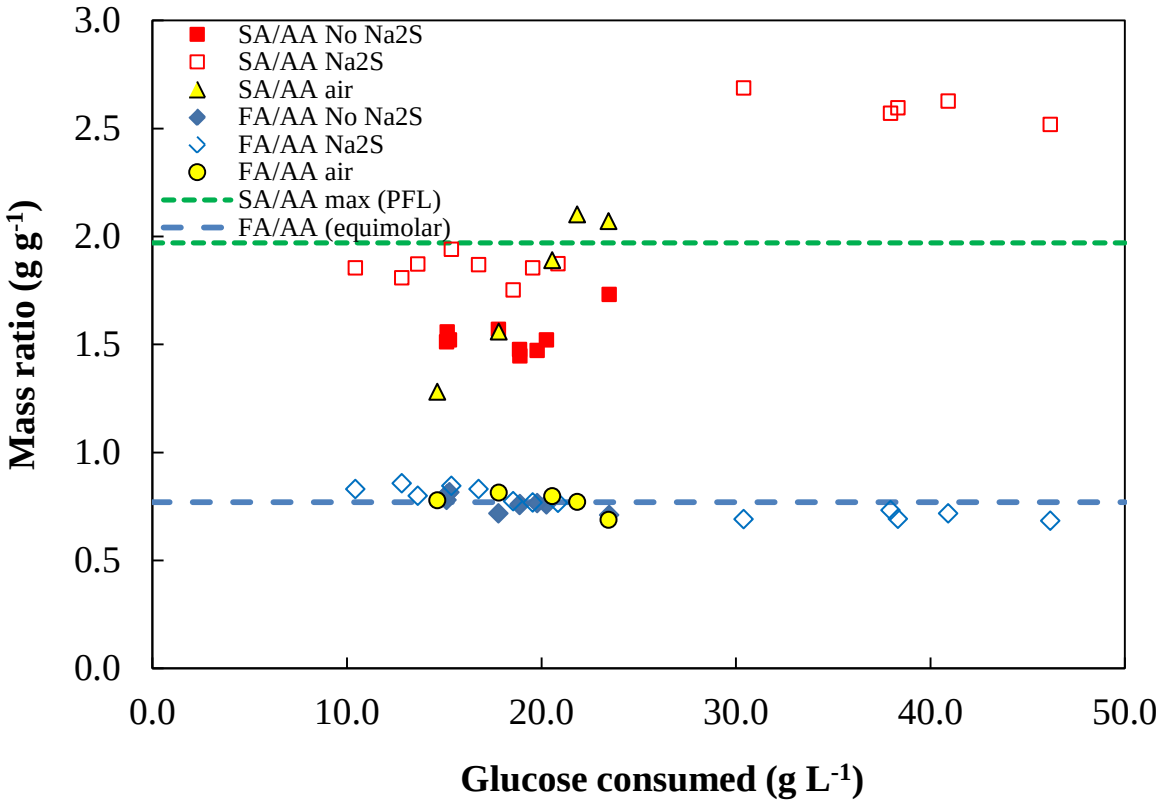

***Figure 4.7**: Product ratios for fermentations using YE-medium. The open and closed squares represent medium with and without $Na_2S{\cdot}9H_2O$ respectively. The broken line at 1.97 g g^{-1} indicates the maximum Y_{AASA} for the PFL pathway. The broken line at 0.77 g g^{-1} represents equimolar formation of FA and AA (PFL pathway).*

Despite Y_{AASA} increasing above 1.97 g g^{-1}, pyruvate conversion proceeded solely via the PFL pathway. The majority of the Y_{AAFA} values lie on the equimolar line (0.77 g g^{-1}) across all values of glucose consumed (Figure 4.7), with only a few points lying marginally below 0.77 g g^{-1} at high glucose consumptions. It was expected that introducing oxygen (as air) into the system would deactivate PFL (Section 2.2.2), forcing *A. succinogenes* to metabolise pyruvate via PDH. Since

Y_{AAFA} remained around 0.77 g g^{-1} with air in the system, PFL deactivation was not observed. However, the concentration of O_2 in the medium may have been insufficient to deactivate an appreciable amount of PFL since the air flow rate was relatively low (approximately 0.02 vvm) and air consists of 21% O_2 by volume.

The constant flux through the PFL pathway suggests that the additional NADH required for C_4 pathway flux, in the case of the higher Y_{AASA} values, was generated elsewhere and not from pyruvate conversion. It is possible that the additional reducing power was generated by the same pathways that generated the additional reducing power for the CSYE-medium runs. The existent biofilm, at the time when the high Y_{AASA} values were obtained, was initially grown on CSYE-medium. Therefore, the cells within the biofilm could contain residual amounts of the components found in the CSYE-medium which would be necessary to activate the alternative metabolic pathways.

Any additional reducing power in the yeast extract would have been detected in the CSYE-medium analysis and the effect would have been more pronounced in the YE-medium fermentations. Therefore, it is unlikely that the medium provides the additional reducing power. It is also unlikely that the additional NADH is provided by biomass synthesis as it was demonstrated in Section 4.2 that biomass contributes an insignificant portion to overall NADH production.

Benefits of CSL

The constant Y_{AAFA} value for the YE-medium fermentations contrasts with the CSYE-medium runs where Y_{AAFA} fell below 0.77 g g^{-1} (Figure 4.2). Therefore, it is possible that the presence of CSL in the fermentation medium activates either the PDH or the FDH pathway. In addition, the Y_{AASA} values obtained in the YE-medium runs were significantly lower than those for the mixed–medium

runs. This suggests that CSL contains an ingredient or combination of ingredients that facilitates SA production beyond the activation of NADH-generating pathways in pyruvate metabolism. Therefore, if the hypothesis is correct that alternative metabolic pathways are active in generating additional reducing power, CSL probably contains co-factors or trace elements crucial to the activation and functioning of these pathways.

Yield on glucose

The yield of SA on glucose, for the YE-medium runs, was below 0.66 g g^{-1} for most of the samples and below 0.87 g g^{-1} for all the samples (Figure 4.8), which compares well with values in the literature for YE-medium fermentations (Table 2.1 and Table 2.2). The highest yield achieved was 0.75 g g^{-1}, which is greater than the highest found in the literature (0.59 g g^{-1}) for a continuous fermentation using YE-medium (Kim et al., 2009).

The yields that were greater than, or equal to, 0.66 g g^{-1} occurred at glucose consumptions above 30 g L^{-1} and correspond to Y_{AASA} values above 1.97 g g^{-1} (Figure 4.7). Yields for situations without $Na_2S{\cdot}9H_2O$ were less than those where $Na_2S{\cdot}9H_2O$ was present; this ties in with O_2 activating oxidative phosphorylation, leading to greater biomass yields, as discussed above. In addition, a trend similar to that for Y_{AASA} was observed for Y_{GLSA} as the CO_2 concentration varied in the presence of air. This is probably associated with glucose being channelled to biomass synthesis instead of SA at higher O_2 concentrations. All the yields were above 0.50 g g^{-1}, which is significantly lower than the baseline for the CSYE-medium fermentations (0.68 g g^{-1}).

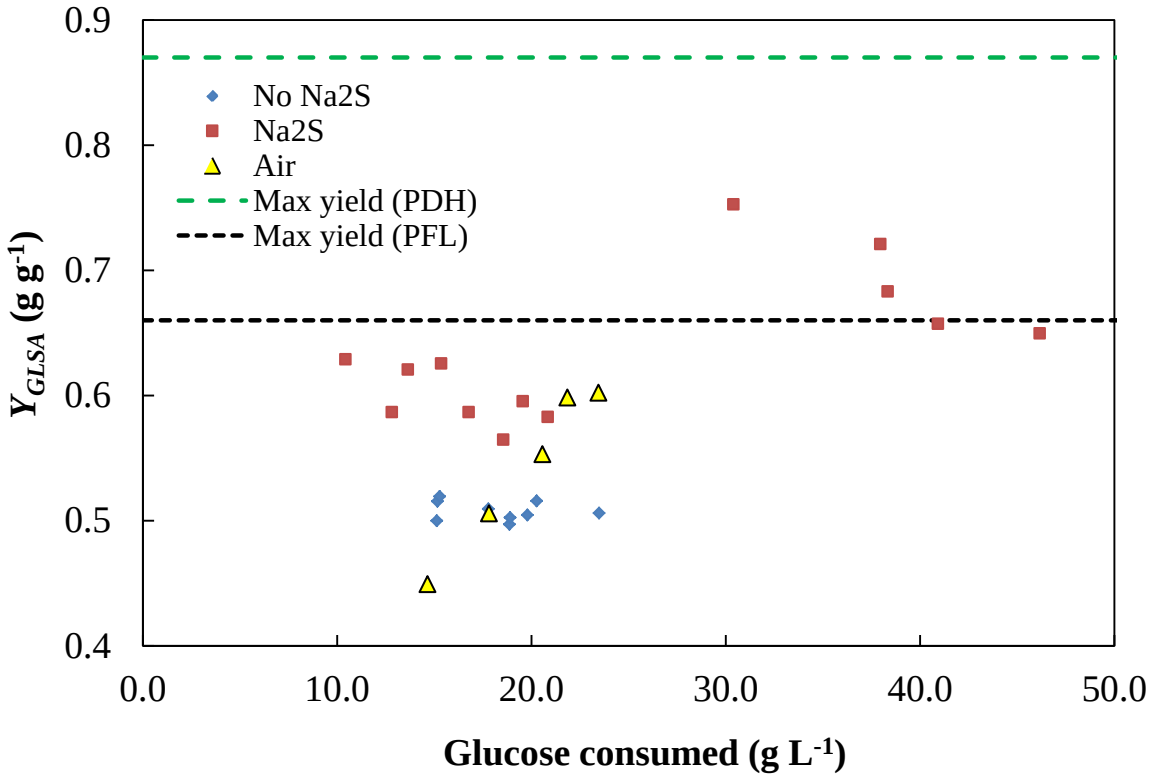

***Figure 4.8**: Yield of succinic acid on glucose for the YE-medium runs. The maximum theoretical yields (broken lines) are 0.66 g g^{-1} (PFL) and 0.87 g g^{-1} (PDH/FDH).*

5. Conclusions

In this study it was found that the steady-state metabolic flux distribution of *A. succinogenes*, grown on a CSL-containing medium, in a continuous biofilm reactor, is a function of glucose consumption. More specifically, C_{SA} increased continuously with increasing glucose consumption, while C_{AA} and C_{FA} flattened out and decreased to zero respectively. Furthermore, succinate production (i.e. flux to the C_4 metabolic pathway) was favoured at high values of glucose consumed, when the organism probably entered a maintenance or non-growth state, thus expressing different metabolic pathways and allowing for greater yields and SA titres.

The theoretical maximum values for Y_{AASA} and Y_{GLSA} were exceeded when CSL was present in the medium, whereas for medium that did not contain CSL these ratios remained within the theoretical limits. The highest Y_{AASA} and Y_{GLSA} for the CSL-containing runs were 5.7 g g^{-1} and 0.91 g g^{-1} respectively. Moreover, Y_{AAFA} was consistently less than 0.77 g g^{-1} (equimolar), approaching zero as C_{FA} decreased, which suggests that either the PDH or the FDH pathway, or a combination thereof, becomes increasingly active with increasing glucose consumption. Y_{AAFA} remained around 0.77 g g^{-1} when CSL was not present in the medium. Therefore, pyruvate metabolism proceeded solely via the PFL pathway in the absence of CSL.

The pathways facilitating lower Y_{AAFA} values for runs containing CSL allow for an increase in Y_{AASA} due to additional NADH generation, but could not account for the total surplus NADH required. The activation of alternative metabolic pathways that generate NADH or the presence of reducing power in the feed medium are possible explanations for the observed excess NADH. The most significant results were achieved in the presence of an established biofilm.

In contrast to the benefits obtained using CSL-containing medium, no significant advantages were observed in the metabolic flux distribution when CSL was excluded (i.e. YE was the only nitrogen source). Yields, productivities and SA concentrations were significantly lower for fermentations that did not contain CSL in the feed.

The highest C_{SA} (48.5 g L^{-1}), q_{SA} (9.4 g L^{-1} h^{-1}), Y_{GLSA} (0.91 g g^{-1}) and glucose conversion (99.4%) attained in this study, all with CSL-containing medium, exceeded the values in the literature for continuous fermentations with *A. succinogenes*. This further supports the commercialisation of bio-based succinic acid using *A. succinogenes* as the catalyst and highlights the potential of using corn steep liquor in the fermentation medium.

Sterility issues encountered in previous studies on *A. succinogenes* were partly overcome in this study with significant fermentations operational for 22 to 57 days. This is partly due to the successful implementation of a technique to replenish the fermentation medium sterilely during continuous operation. In addition, problems of excessive foam and entrainment were partially dealt with by introducing a liquid-free reactor headspace, adding antifoam directly to the fermentation medium and providing controlled, online antifoam dosing.

6. Recommendations

In this study, the best yields, productivities and titres were achieved in the presence of an established biofilm. This highlights the importance of biofilm in enhancing bioreactor performance. Therefore, it is important to determine optimal methods and materials to immobilise *A. succinogenes*, thereby increasing cell density in the reactor. Such an optimisation necessitates accurate determination of the total biomass content in the reactor as this allows for the development of a kinetic model, which is essential for scale-up.

The variations in metabolic flux reported in this study are encouraging as they hint that wild-type *A. succinogenes* can perform beyond its expected capabilities. This bolsters its position as a candidate for commercial succinate production. However, to utilise this potential to the full it is essential to determine the metabolic pathway that affords the high ratios of succinate to acetate and produces the surplus NADH used in the C_4 pathway.

The significantly better results attained with medium containing corn steep liquor (CSL) motivate its use as a component in an industrial feed. It is essential to understand fully why CSL leads to dramatic improvements in succinic acid production and under what conditions this occurs. Furthermore, it is important to determine the identity of the ‘wonder’ ingredient in CSL as this will allow optimisation of the fermentation medium which could reduce fermentation costs and make bio-based succinate production with *A. succinogenes* commercially feasible.

7. References

Beauprez, JJ, De Mey, M & Soetaert, WK (2010) "Microbial succinic acid production: Natural versus metabolic engineered producers", *Process Biochemistry*, 45 (7), 1103–1114.

Bozell, JJ & Petersen, GR (2010) "Technology development for the production of biobased products from biorefinery carbohydrates—the US Department of Energy's 'Top 10' revisited", *Green Chemistry*, 12 (4), 539.

Corona-González, RI, Bories, A, González-Álvarez, V & Pelayo-Ortiz, C (2008) "Kinetic study of succinic acid production by *Actinobacillus succinogenes* ZT-130", *Process Biochemistry*, 43 (10), 1047–1053.

Corona-Gonzalez, RI, Bories, A, González-Alvarez, V, Snell-Castro, R, Toriz-González, G & Pelayo-Ortiz, C (2010) "Succinic acid production with *Actinobacillus succinogenes* ZT-130 in the presence of succinic acid", *Current microbiology*, 60 (1), 71–7.

DeJong, E, Higson, A, Walsh, P & Wellisch, M (2012) "Product developments in the bio-based chemicals arena", *Biofuels, Bioproducts and Biorefining*, 6 , 606–624.

Du, C, Lin, SKC, Koutinas, A, Wang, R, Dorado, P & Webb, C (2008) "A wheat biorefining strategy based on solid-state fermentation for fermentative production of succinic acid", *Bioresource technology*, 99 (17), 8310–5.

Fernando, S, Adhikari, S, Chandrapal, C & Murali, N (2006) "Biorefineries: Current Status, Challenges, and Future Direction", *Energy & Fuels*, 20 (4), 1727–1737.

Guettler, M, Jain, M & Rumler, D (1996) "Method for making succinic acid, bacterial variants for use in the process, and methods for obatining variants", USA, *5,573,931*.

Guettler, M, Jain, M & Soni, B (1998) "Process for making succinic acid, microorganisms for use in the process and methods of obtaining the microorganisms", USA, *US005723322A*.

Guettler, M, Rumler, D & Jain, M (1999) "*Actinobacillus succinogenes* sp. nov., a novel succinic-acid-producing strain from the bovine rumen", *International Journal of Systematic Bacteriology*, 49 , 207–216.

Kim, M Il, Kim, N-J, Shang, L, Chang, YK, Lee, SY & Chang, HN (2009) "Continuous Production of Succinic Acid Using an External Membrane Cell Recycle System", *Journal of Microbiology and Biotechnology*, 19 (11), 1369–1373.

Knappe, J, Neugebauert, FA, Blaschkowski, HP & Ganzler, M (1984) "Post-translational activation introduces a free radical into pyruvate formate-lyase", *Proceedings of the National Academy of Sciences of the United States of America*, 81 (March), 1332–1335.

Lee, PC, Lee, SY, Hong, SH & Chang, HN (2002) "Isolation and characterization of a new succinic acid-producing bacterium, *Mannheimia succiniciproducens* MBEL55E, from bovine rumen.", *Applied microbiology and biotechnology*, 58 (5), 663–8.

Lee, PC, Lee, WG, Kwon, S, Lee, SY & Chang, HN (2000) "Batch and continuous cultivation of *Anaerobiospirillum succiniciproducens* for the production of succinic acid from whey", *Applied microbiology and biotechnology*, 54 (1), 23–7.

Lin, H, Bennett, GN & San, K-Y (2005) "Fed-batch culture of a metabolically engineered *Escherichia coli* strain designed for high-level succinate production and yield under aerobic conditions", *Biotechnology and bioengineering*, 90 (6), 775–9.

Lin, SKC, Du, C, Koutinas, A, Wang, R & Webb, C (2008) "Substrate and product inhibition kinetics in succinic acid production by *Actinobacillus succinogenes*", *Biochemical Engineering Journal*, 41 (2), 128–135.

Liu, Y-P, Zheng, P, Sun, Z-H, Ni, Y, Dong, J-J & Zhu, L-L (2008) "Economical succinic acid production from cane molasses by *Actinobacillus succinogenes*", *Bioresource technology*, 99 (6), 1736–42.

Markets-and-Markets (2012) *Succinic Acid Market by Applications & Geography - Global Trends & Forecasts (2011 - 2016)*, http://www.marketsandmarkets.com/market-reports/succinic-acid-market-402.html.

McKinlay, JB, Laivenieks, M, Schindler, BD, McKinlay, A a, Siddaramappa, S, Challacombe, JF, Lowry, SR, Clum, A, Lapidus, AL, Burkhart, KB, et al. (2010) "A genomic perspective on the potential of *Actinobacillus succinogenes* for industrial succinate production.", *BMC genomics*, 11 (1), 680.

McKinlay, JB, Shachar-Hill, Y, Zeikus, JG & Vieille, C (2007) "Determining *Actinobacillus succinogenes* metabolic pathways and fluxes by NMR and GC-MS analyses of 13C-labeled metabolic product isotopomers", *Metabolic engineering*, 9 (2), 177–92.

McKinlay, JB, Zeikus, JG & Vieille, C (2005) "Insights into *Actinobacillus succinogenes* fermentative metabolism in a chemically defined growth medium", *Applied and environmental microbiology*, 71 (11), 6651–6.

Nielsen, J (1998) "Metabolic engineering: techniques for analysis of targets for genetic manipulations", *Biotechnology and bioengineering*, 58 (2-3), 125–32.

Oh, I, Lee, H, Park, C, Lee, SY & Lee, J (2008) "Succinic acid production by continuous fermentation process using *Mannheimia succiniciproducens* LPK7", *Journal of Microbiology and Biotechnology*, 18 (5), 908–912.

Park, DH & Zeikus, JG (1999) "Utilization of electrically reduced neutral red by *Actinobacillus succinogenes*: physiological function of neutral red in membrane-driven fumarate reduction and energy conservation.", *Journal of bacteriology*, 181 (8), 2403–10.

Reverdia (2011) “Reverdia Technology: Low pH Yeast Production Provides Significant Environmental and Quality Advantages”, viewed 4 October, 2013, <http://www.reverdia.com/technology/>, http://www.reverdia.com/technology/.

Rühl, M, Le Coq, D, Aymerich, S & Sauer, U (2012) “13C-flux analysis reveals NADPH-balancing transhydrogenation cycles in stationary phase of nitrogen-starving *Bacillus subtilis*”, *The Journal of biological chemistry*, 287 (33), 27959–70.

Samuelov, NS, Lamed, R, Lowe, S & Zeikus, JG (1991) “Influence of CO(2)-HCO(3) Levels and pH on Growth, Succinate Production, and Enzyme Activities of *Anaerobiospirillum succiniciproducens*.”, *Applied and environmental microbiology*, 57 (10), 3013–9.

Scholten, E, Renz, T & Thomas, J (2009) “Continuous cultivation approach for fermentative succinic acid production from crude glycerol by *Basfia succiniciproducens* DD1.”, *Biotechnology letters*, 31 (12), 1947–51.

Segel, L & Slemrod, M (1989) “The quasi-steady-state assumption: a case study in perturbation”, *SIAM review*, 31 (3), 446–477.

Song, H & Lee, SY (2006) “Production of succinic acid by bacterial fermentation”, *Enzyme and Microbial Technology*, 39 (3), 352–361.

Spector, MP (2009) “Metabolism, Central (Intermediary)” in , E-CM Schaechter (ed.) , *Encyclopedia of Microbiology (Third Edition)*Third Edit., Academic Press, Oxford, 242–264.

Stewart, PS & Franklin, MJ (2008) “Physiological heterogeneity in biofilms”, *Nature reviews. Microbiology*, 6 (3), 199–210.

Transparency-Market-Research (2013) *Succinic Acid Market for 1,4-BDO, Resin, Coatings, Dyes & Inks, Pharmaceutical, Polyurethane, Food, Plasticizers, Cosmetics, Solvents & Lubricants and De-Icing Solutions Applications - Global Industry Analysis, Size, Share, Growth, Trends and Forecast, 20*, http://www.transparencymarketresearch.com/succinic-acid.html.

Urbance, SE, Pometto, AL, DiSpirito, A a. & Demirci, A (2003) “Medium Evaluation and Plastic Composite Support Ingredient Selection for Biofilm Formation and Succinic Acid Production by *Actinobacillus succinogenes*”, *Food Biotechnology*, 17 (1), 53–65.

Urbance, SE, Pometto, AL, Dispirito, A a & Denli, Y (2004) “Evaluation of succinic acid continuous and repeat-batch biofilm fermentation by *Actinobacillus succinogenes* using plastic composite support bioreactors”, *Applied microbiology and biotechnology*, 65 (6), 664–70.

van der Werf, MJ, Guettler, M V, Jain, MK & Zeikus, JG (1997) “Environmental and physiological factors affecting the succinate product ratio during carbohydrate fermentation by *Actinobacillus* sp. 130Z”, *Archives of microbiology*, 167 (6), 332–42.

van Heerden, CD & Nicol, W (2013a) “Continuous succinic acid fermentation by *Actinobacillus succinogenes*”, *Biochemical Engineering Journal*, 73 , 5–11.

van Heerden, CD & Nicol, W (2013b) “Continuous and batch cultures of *Escherichia coli* KJ134 for succinic acid fermentation: metabolic flux distributions and production characteristics.”, *Microbial cell factories*, 12 (1), 80.

VijayaVenkata Raman, S, Iniyan, S & Goic, R (2012) “A review of climate change, mitigation and adaptation”, *Renewable and Sustainable Energy Reviews*, 16 (1), 878–897.

Villadsen, J, Nielsen, J & Lidén, G (2011) *Bioreaction Engineering Principles*Third., Springer US, Boston, MA.

Wagner, AF, Frey, M, Neugebauer, FA, Schäfer, W & Knappe, J (1992) “The free radical in pyruvate formate-lyase is located on glycine-734.”, *Proceedings of the National Academy of Sciences of the United States of America*, 89 (3), 996–1000.

Werpy, T & Petersen, G (2004) *Top value added chemicals from biomass, Volume 1. Results of screening for potential candidates from sugars and synthesis gas*.

Wöltinger, J, Karau, A, Leuchtenberger, W & Drauz, K (2005) “Membrane Reactors at Degussa”, *Adv Biochem Engin/Biotechnol*, 92 , 289–316.

Xi, Y, Chen, K, Dai, W, Ma, J, Zhang, M, Jiang, M, Wei, P & Ouyang, P-K (2013) “Succinic acid production by *Actinobacillus succinogenes* NJ113 using corn steep liquor powder as nitrogen source”, *Bioresource technology*, 136 , 775–9.

Xi, Y, Chen, K, Xu, R, Zhang, J, Bai, X, Jiang, M, Wei, P & Chen, J (2012) “Effect of biotin and a similar compound on succinic acid fermentation by *Actinobacillus succinogenes* in a chemically defined medium”, *Biochemical Engineering Journal*, 69 , 87–92.

Zeikus, JG, Jain, MK & Elankovan, P (1999) “Biotechnology of succinic acid production and markets for derived industrial products”, *Applied Microbiology and Biotechnology*, 51 (5), 545–552.

Appendices

Appendix A: CSYE-medium data

R*	D (h^{-1})	C_{GL} (g L^{-1})	C_{GLe} (g L^{-1})	ΔGL (g L^{-1})	C_{SA} (g L^{-1})	C_{AA} (g L^{-1})	C_{FA} (g L^{-1})	DCW (g L^{-1})	Y_{AASA} (g g^{-1})	Y_{AAFA} (g g^{-1})	Y_{GLSA} (g g^{-1})	γ	q_{SA} (g L^{-1} h^{-1})	CO_2 (vvm)	Air (vvm)
B	0.11	31.0	29.1	28.5	21.0	7.0	2.8	0.4	3.02	0.41	0.74	0.98	2.2	0.10	0
	0.11	31.0	29.1	29.0	21.9	6.9	2.6	0.5	3.19	0.37	0.76	0.99	2.3	0.05	0
	0.34	31.0	29.2	25.9	19.7	5.9	2.9		3.32	0.49	0.77	0.89	6.7	0.05	0
	0.33	31.0	29.3	19.4	14.2	4.5	2.7		3.17	0.61	0.74	0.66	4.7	0.10	0
	0.22	61.4	58.5	24.9	16.9	4.7	2.7		3.60	0.57	0.70	0.43	3.8	0.05	0
	0.23	61.4	58.2	26.1	20.3	5.4	2.5		3.75	0.47	0.80	0.45	4.6	0.05	0
	0.11	61.4	56.5	45.9	38.6	6.8	0.2		5.70	0.03	0.85	0.81	4.2	0.05	0
	0.09	61.4	55.7	45.6	40.7	7.3	0.2		5.57	0.03	0.90	0.82	3.7	0.05	0
	0.10	61.4	57.7	27.9	24.2	6.3	2.0		3.86	0.32	0.89	0.48	2.4	0.05	0
	0.08	61.4	57.8	28.4	21.9	6.1	2.3		3.59	0.38	0.79	0.49	1.7	0.03	0
	0.05	61.4	56.6	37.0	28.6	6.8	1.4		4.21	0.21	0.78	0.65	1.5	0.03	0
	0.04	61.4	55.3	38.5	33.3	7.4	1.1		4.50	0.15	0.88	0.70	1.2	0.03	0

R*	D (h^{-1})	C_{GL} (g L^{-1})	C_{GLe} (g L^{-1})	ΔGL (g L^{-1})	C_{SA} (g L^{-1})	C_{AA} (g L^{-1})	C_{FA} (g L^{-1})	DCW (g L^{-1})	Y_{AASA} (g g^{-1})	Y_{AAFA} (g g^{-1})	Y_{GLSA} (g g^{-1})	γ	q_{SA} (g L^{-1} h^{-1})	CO_2 (vvm)	Air (vvm)
	0.05	61.4	56.8	41.0	33.6	7.5	0.9	0.1	4.51	0.12	0.83	0.72	1.8	0.03	0
	0.05	61.4	56.8	41.9	33.6	7.5	1.0		4.46	0.14	0.81	0.74	1.8	0.03	0
	0.05	61.4	57.1	41.4	33.9	7.4	1.1	0.4	4.56	0.14	0.83	0.73	1.8	0.03	0
	0.33	61.4	59.5	18.5	12.9	4.1	2.5		3.11	0.60	0.72	0.31	4.2	0.05	0
	0.32	60.3	57.6	19.4	13.7	4.6	2.9	4.5	2.96	0.63	0.71	0.34	4.4	0.05	0
	0.33	60.3	58.3	15.2	10.4	4.2	3.0		2.50	0.73	0.70	0.26	3.4	0.10	0
B	0.04	60.3	54.5	40.0	30.8	7.7	2.3		4.00	0.30	0.77	0.73	1.2	0.05	0
	0.05	60.3	55.8	39.1	30.2	7.7	2.2		3.94	0.29	0.78	0.70	1.4	0.05	0
	0.05	60.3	56.5	36.3	28.7	7.4	2.1	3.2	3.87	0.28	0.80	0.64	1.4	0.05	0
	0.11	60.3	57.7	19.0	13.2	5.2	3.2		2.55	0.62	0.70	0.33	1.4	0.08	0
	0.10	60.3	57.6	20.0	13.8	5.4	3.4	2.3	2.56	0.64	0.70	0.35	1.4	0.05	0
	0.17	26.0	25.2	18.8	13.6	5.2	3.0	1.7	2.62	0.59	0.74	0.74	2.3	0.06	0
	0.54	68.9	65.9	23.2	17.5	5.1	3.1		3.44	0.61	0.77	0.35	9.4	0.06	0
	0.11	68.9	61.4	55.3	45.8	9.3	1.1		4.93	0.12	0.84	0.90	5.1	0.11	0

R*	D (h^{-1})	C_{GL} (g L^{-1})	C_{GLe} (g L^{-1})	ΔGL (g L^{-1})	C_{SA} (g L^{-1})	C_{AA} (g L^{-1})	C_{FA} (g L^{-1})	DCW (g L^{-1})	Y_{AASA} (g g^{-1})	Y_{AAFA} (g g^{-1})	Y_{GLSA} (g g^{-1})	γ	q_{SA} (g L^{-1} h^{-1})	CO_2 (vvm)	Air (vvm)
B	0.07	68.9	62.9	57.9	48.5	9.6	0.2	0.3	5.05	0.02	0.84	0.92	3.2	0.11	0
	0.11	60.3	56.5	36.3	30.9	6.8	0.7	0.5	4.53	0.11	0.86	0.64	3.3	0.11	0
	0.11	60.3	56.6	34.7	27.8	6.3	1.3		4.41	0.21	0.81	0.61	3.0	0.05	0
	0.10	60.3	54.5	28.9	21.9	6.6	3.5		3.34	0.53	0.77	0.53	2.2	0.11	0
	0.11	60.3	55.1	32.6	25.1	7.1	3.6		3.53	0.50	0.78	0.59	2.8	0.11	0
	0.04	59.8	49.1	40.1	36.0	8.0	3.4	0.5	4.51	0.42	0.91	0.82	1.5	0.11	0
	0.05	59.8	50.3	41.3	34.5	8.1	4.0		4.23	0.49	0.84	0.82	1.6	0.11	0
	0.05	59.8	50.9	41.7	33.8	8.7	4.5		3.90	0.51	0.82	0.82	1.7	0.11	0
	0.06	59.8	51.9	42.5	33.7	8.9	4.7		3.78	0.52	0.80	0.82	1.9	0.11	0

*Reactor

Appendix B: YE-medium data

R*	D (h^{-1})	C_{GL} (g L^{-1})	C_{GLe} (g L^{-1})	ΔGL (g L^{-1})	C_{SA} (g L^{-1})	C_{AA} (g L^{-1})	C_{FA} (g L^{-1})	DCW (g L^{-1})	Y_{AASA} (g g^{-1})	Y_{AAFA} (g g^{-1})	Y_{GLSA} (g g^{-1})	γ	q_{SA} (g L^{-1} h^{-1})	CO_2 (vvm)	Air (vvm)	†Na_2S
A	0.05	30.5	28.8	23.5	11.9	6.9	4.9		1.73	0.71	0.51	0.82	0.6	0.011	0	No
	0.07	30.5	29.4	17.8	9.1	5.8	4.1		1.57	0.72	0.51	0.61	0.6	0.007	0	No
	0.09	30.5	29.2	18.9	9.4	6.4	4.8		1.48	0.76	0.50	0.65	0.9	0.011	0	No
	0.10	30.5	29.0	18.9	9.5	6.6	5.0	2.9	1.45	0.76	0.50	0.65	0.9	0.011	0	No
	0.20	30.5	29.6	15.1	7.6	5.0	3.9		1.51	0.78	0.50	0.51	1.5	0.015	0	No
	0.19	30.5	29.4	15.2	7.8	5.0	4.0	2.9	1.56	0.81	0.52	0.51	1.5	0.015	0	No
	0.19	30.5	29.4	15.3	7.9	5.2	4.3	2.6	1.52	0.81	0.52	0.52	1.5	0.015	0	No
	0.10	30.5	29.1	20.3	10.5	6.9	5.2		1.52	0.76	0.52	0.70	1.0	0.011	0	No
	0.09	30.5	29.2	19.8	10.0	6.8	5.2	2.4	1.47	0.76	0.50	0.68	0.9	0.011	0	No
B	0.11	29.8	28.3	18.56	10.3	5.9	4.5		1.75	0.77	0.56	0.66	1.1	0.10	0	Yes
	0.12	29.8	28.2	10.43	6.3	3.4	2.8		1.85	0.83	0.63	0.37	0.8	0.10	0	Yes

R*	D (h^{-1})	C_{GL} (g L^{-1})	C_{GLe} (g L^{-1})	ΔGL (g L^{-1})	C_{SA} (g L^{-1})	C_{AA} (g L^{-1})	C_{FA} (g L^{-1})	DCW (g L^{-1})	Y_{AASA} (g g^{-1})	Y_{AAFA} (g g^{-1})	Y_{GLSA} (g g^{-1})	γ	q_{SA} (g L^{-1} h^{-1})	CO_2 (vvm)	Air (vvm)	†Na_2S
	0.11	29.8	27.8	19.56	11.4	6.2	4.7	2.17	1.85	0.77	0.60	0.70	1.3	0.10	0	Yes
	0.10	29.8	27.8	20.85	11.9	6.4	4.9	1.96	1.87	0.77	0.58	0.75	1.2	0.10	0	Yes
	0.20	29.8	28.1	13.65	8.3	4.4	3.5		1.87	0.80	0.62	0.49	1.7	0.10	0	Yes
	0.25	29.8	28.3	16.78	9.6	5.2	4.3	2.37	1.87	0.83	0.59	0.59	2.5	0.10	0	Yes
	0.34	29.8	28.6	12.82	7.3	4.0	3.5		1.81	0.86	0.59	0.45	2.6	0.10	0	Yes
B	0.31	29.8	28.3	15.37	9.4	4.8	4.1	1.61	1.94	0.85	0.63	0.54	3.0	0.10	0	Yes
	0.09	60.6	51.7	30.40	22.4	8.4	5.8		2.69	0.69	0.75	0.59	2.1	0.17	0	Yes
	0.12	60.6	54.5	38.34	25.7	9.9	6.9		2.60	0.69	0.68	0.70	3.1	0.04	0	Yes
	0.12	60.6	53.9	40.93	26.4	10.1	7.2		2.63	0.72	0.66	0.76	3.1	0.085	0	Yes
	0.12	60.6	53.2	37.96	26.9	10.5	7.7		2.57	0.73	0.72	0.71	3.1	0.085	0	Yes
	0.06	60.6	51.2	46.17	29.5	11.7	8.0		2.52	0.68	0.65	0.90	1.9	0.04	0	Yes
	0.19	30.4	29.5	14.7	6.6	5.1	4.0		1.28	0.78	0.45	0.50	1.3	0.017	0.59	No
A	0.20	30.4	29.2	17.8	9.0	5.8	4.7		1.56	0.81	0.51	0.61	1.8	0.024	0.22	No
	0.21	30.4	28.8	23.5	14.1	6.8	4.7		2.07	0.69	0.60	0.81	2.9	0.035	0.22	No

R*	D (h^{-1})	C_{GL} (g L^{-1})	C_{GLe} (g L^{-1})	ΔGL (g L^{-1})	C_{SA} (g L^{-1})	C_{AA} (g L^{-1})	C_{FA} (g L^{-1})	DCW (g L^{-1})	Y_{AASA} (g g^{-1})	Y_{AAFA} (g g^{-1})	Y_{GLSA} (g g^{-1})	γ	q_{SA} (g L^{-1} h^{-1})	CO_2 (vvm)	Air (vvm)	†Na_2S
	0.34	30.4	29.0	20.6	11.4	6.0	4.8		1.89	0.80	0.55	0.71	3.9	0.045	0.22	No
	0.31	30.4	29.2	21.8	13.1	6.2	4.8		2.10	0.77	0.60	0.75	4.1	0.040	0.22	No

*Reactor; †$Na_2S \cdot 9H_2O$